A Review of the Dynamics and Oscillations of the Atmosphere

A thesis

submitted in partial fulfilment

of the requirements for the Degree

of

Master of Science

at the

University of Waikato

by

Joseph Ross

THE UNIVERSITY OF
WAIKATO
Te Whare Wānanga o Waikato

University of Waikato

2012

Abstract

The atmosphere is a complex, dynamic system and the weather depends on its state. There are many different phenomena that affect the state of the atmosphere - some only involve the atmosphere, others involve the interaction between the atmosphere and the ocean. These phenomena can be modelled using many equations originating from fluid dynamics and thermodynamics, and many of them are considered here. Energy travels around the atmosphere in the form of planetary waves, such as Kelvin waves and Rossby waves. It is possible for a triad of Rossby waves to interact with each other in a way such that resonance occurs. A computer simulation investigating the sensitivity of such waves to turbulence was completed, and it was found that the energetic dominance of the resonant triad does not persist, and the greater the turbulence added to the Rossby triad, the earlier in the integration the instabilities occur.

Acknowledgements

I would like to thank my supervisor, Sean Oughton, whose expertise, encouragement and feedback made it easier to find the necessary motivation to continue the research required to put this document together.

Thank you to Peter Lynch, an employee of Met Éireann at the time he completed the relevant work, who responded to my questions about his work in a timely manner, and clarified some points about his MATLAB code.

A thank you must also go to some of my fellow graduate students, Will Crump and Ben O'Neil who helped with a couple of issues I had with LaTeX at the beginning of the writing, and also to Matt Ussher, who gave me some feedback on the introduction.

Contents

Chapter 1

Introduction

The Earth is surrounded by an atmosphere, a concoction of gases which is gravitationally attracted to the Earth. This atmosphere plays a crucial role in maintaining life on Earth as there would be no life possible on land without the oxygen in the atmosphere.

In this thesis, we will discuss fluid dynamics and obtain the Navier-Stokes equation and the equations of the atmosphere. This will require some use of the theory of thermodynamics. We will look at Planetary Waves (Rossby and Kelvin waves) and analyse the mechanisms of the El Niño Southern Oscillation that gives rise to the phenomena of El Niño and La Niña.

Without the atmosphere there would be no weather patterns on Earth as we know them. Weather on Earth ranges from calm to catastrophic, from dour to dramatic. And the weather patterns on Earth are caused by the atmosphere transferring energy from one part of the Earth to another, in its constant battle to reach equilibrium. It never does succeed in achieving this equilibrium, for the tropics receive more direct sunlight than the poles do. This is due to the curvature of the Earth, and results in a large variation of temperature and air pressure with latitude. As a result, it is at times unbearably hot near the equator, but unbearably cold at the poles. Temperatures often exceed 40° C

near the equator during the day, and have been known to drop as low as -88° C in Antarctican winter. It is very little wonder then that Antarctica is largely unpopulated during the winter months!

The atmosphere acts to reduce the gradient of temperature and pressure by transferring energy from areas of high energy to areas of low energy. One mechanism that reduces the gradient is wind. Wind always blows from areas of high pressure to areas of low pressure in an attempt to balance out the pressure gradient - the larger the gradient, the stronger the wind.

The weather is of great importance to all life on earth, not just the human race. Deciduous trees lose their leaves in autumn and regrow them in spring. Many animals hibernate during the coldest weather, to arise in spring. Numerous species of plants only flower at a particular time of the year, when the weather conditions are optimal for that species.

Humans also need to know what the weather is going to be for the immediate future, for a variety of reasons. It could be to decide whether they should take their umbrella to work. On other occasions it is about whether their recreation plans are likely to go ahead, and what the conditions are likely to be, so they can prepare accordingly. But for many more, their livelihood is at stake. Those who make their living growing fruit are particularly at the mercy of the weather. This is why tomatoes are grown in glasshouses, where they can control the conditions. But for growers of other products, this is not practical. Many vineyards use helicopters to protect their crops from frosts, since frost destroys the fruits of their labour, and the blades of the helicopter disturb the air enough to prevent the water vapour it is carrying from freezing on the ground.

Life as we know it would not be possible without the weather patterns on

Earth. Much of human life is at the mercy of the weather, so it is in our best interests to understand how it works, because the more we know about the science of weather, the more accurately we can predict it. It therefore comes as very little suprise that weather prediction is a major global industry, with the governments of most major nations devoting a large quantity of resources to this industry, known as *meteorology*.

Meteorology is the science of the atmosphere and the weather. Anyone hoping to enter this field must develop an understanding of the mechanics of the atmosphere, including how energy travels around it and how it carries water vapour. As is the case with most modern sciences, there is a qualitative part of meteorology (What happens? How? Why?) but there is also a quantitative part (How much of an effect does this have? Over what kind of time period does it happen? and other questions that require a quantity of some description to answer them.). Mathematics is required to answer the quantitative questions, and it is also needed to answer some of the qualitative questions, a simulation can give some enormous insight into the phemomena in the atmosphere. So too can the analysis of the equations obeyed by the atmosphere.

There are several phenomena that contribute to weather patterns on Earth, or indeed any planet with a fluid (i.e. liquified or gaseous) atmosphere. As liquids and gases are fluids, the governing physics of the atmosphere are those belonging to the field of fluid dynamics. Energy is transferred by wind as was mentioned earlier, but this is just one of multiple mechanisms that are responsible for the transfer of energy from one part of the atmosphere to another. Wind involves the transfer of matter, of air molecules, from one place to another (In order to decrease pressure gradients, matter must be transferred from an area of high pressure, which means a high number of molecules per unit volume) to an area of lower pressure. However there are two components to

pressure, one is the temperature. As warmer temperature means the molecular movement of air (in this case) is faster, this will also increase the pressure. In order to equalise the pressure in this case, it is necessary for the atmosphere to move some of the energy (which is in the form of molecular kinetic energy) to areas which are cooler (typically towards the poles). This may not involve a migration of mass, just a migration of energy, and such an energy transfer takes place in the form of waves.

This transfer of energy from warmer parts to colder parts of the atmosphere is just like what happens in the ocean. It is well known that currents develop in the ocean due to a migration of mass around the globe due to this temperature gradient, and perhaps the most famous example is the thermohaline conveyor. In the ocean too, energy is transferred from areas of high energy to low energy in the form of planetary waves - waves that travel around the planet. There are several types of planetary wave. In this paper, we shall concentrate on just two main types, the Rossby wave and the Kelvin wave.

The Earth is constantly accelerating - it is orbiting the sun. As it does so, it constantly changes direction as it revolves around the sun. But, as far as the atmosphere is concerned, of greater significance is the acceleration, and therefore force that arises as a result of the Earth's rotation about its own axis. This force is a fictitious force, meaning it only arises in non-inertial reference frames like those attached to the surface of the earth, and therefore could not be felt by an observer on a stationary frame in outer space. However its effects on the atmosphere are blatant - the Coriolis force gives rise to the swirling of cloud matter in the atmosphere that can be seen in satellite imagery. It is this force that generates the rotation seen in cyclones, and can create destructive weather events like tornados and hurricanes that can be devastating to human life.

The atmosphere has many naturally occurring cycles, some of which are global, and some of which are localised to a relatively small geographic region. One of these is the El Niño Southern Oscillation, which takes place in the Pacific Ocean. It is a process that repeats itself every few years, and is responsible for periods of low rainfall and drought in some years and high rainfall and drought in other years. These conditions are typically felt in nations that border the western and eastern edges of the Pacific Ocean (i.e. those such as Australia and nations on the west coast of South America). Such processes can be damaging to crops, upon which many human livelihoods rely. The processes and predictability of ENSO are topics which generate a lot of interest from atmospheric researchers and meteorologists.

Chapter 2

Equations for the Atmosphere

2.1 General Fluid Dynamics

The atmosphere, which along with the ocean is responsible for driving the Earth's weather systems, is a fluid. It therefore must obey the equations of fluid dynamics. There are three fundamental equations of fluid dynamics, which can be derived using conservation of the fundamental quantities mass, momentum and energy respectively.

Since mass is conserved, the rate of change of mass inside a particular volume element must be equal to the inward flux of mass through the boundaries of that volume element. This observation results in the equation

$$\frac{\partial \rho}{\partial t} + \nabla \cdot (\rho \mathbf{v}) = \mathbf{0} \tag{2.1}$$

where ρ is the density of the fluid and $\mathbf{v}$ is its velocity field. This equation can be written in the equivalent form

$$\frac{D\rho}{Dt} + \rho \nabla \cdot \mathbf{v} = \mathbf{0} \tag{2.2}$$

where $\frac{D}{Dt} = \frac{\partial}{\partial t} + \mathbf{v} \cdot \nabla$ is the Lagrangian derivative.

Provided no external forces are applied to the volume element in question, momentum must also be conserved. In general, the fluid must obey Newton's Second Law. From this, it is possible to derive the equation

$$\rho \frac{Dv_i}{Dt} = F_i + \frac{\partial T_{ij}}{\partial x_j} \tag{2.3}$$

This equation is just a statement of Newton's Second Law per unit mass. v_i is the fluid element's velocity in the ith direction, F_i is the body force acting on the fluid element in the ith direction and T_{ij} is the ijth element of the stress tensor, which denotes the force acting on the surface of the fluid element by neighbouring fluid elements (see below).

The body forces are long range forces that act on the whole fluid element (considered infinitesimally small in size, so that the variation of a body force over space is relatively slow).

The surface forces associated with the stress tensor act over small distances, meaning these forces only apply to the surface of the fluid element in consideration. T_{ij}, the ijth element of the stress tensor, gives an indication of the component of the stress in the direction of the $\hat{j}$ unit vector on the surface element of the fluid which has its normal in the direction of the $\hat{i}$ unit vector.

The energy of the fluid element must also be conserved. Taking the dot product with Equation 2.3 and integrating over the volume of the fluid element yields

$$\frac{D}{Dt}\int_V \frac{1}{2}\rho(\mathbf{v})^2 = \int_V \mathbf{v}\cdot\mathbf{F}dV - \int_V T_{ij}\frac{\partial v_i}{\partial x_j}dV + \oint v_i T_{ij} dS_j \qquad (2.4)$$

This equation tells us that the rate of change of kinetic energy of the fluid element is equal to the rate at which the force F does work, minus the dissipation rate (the rate at which the energy is converted to heat energy) plus the work rate of the internal stresses on the surface.

These three equations lead directly to the well-known fundamental equation of fluid mechanics, the Navier-Stokes equation for incompressible fluids (i.e $\nabla\cdot\mathbf{v} = \mathbf{0}$) that have uniform density

$$\frac{\partial \mathbf{v}}{\partial t} + \mathbf{v}\cdot\nabla\mathbf{v} = -\nabla p + \frac{\mu}{\rho}\nabla^2\mathbf{v} + \mathbf{F} \qquad (2.5)$$

where p is the pressure and μ the viscosity.
Ideally, the atmosphere is an example of a density stratified fluid, since the pressure and density decrease as a function of height only. At ground level, the atmosphere has a typical density of 1.2 to 1.3 kg m^{-3}. But the pressure of the atmosphere is never horizontally uniform over large distance scales. These differences in pressure lead to the wind, which blows from areas of high pressure to areas of low pressure.

Note that we have some nonlinear terms in the Navier-Stokes equation. In fluids with nonzero viscosity (i.e. all fluids except superfluids. An example of superfluids is ^{3}He in temperatures below about 2 Kelvin), there will be examples of nonlinear behaviour. These fluids include the atmosphere, which behaves in a very nonlinear fashion. This makes the weather difficult to predict, since these nonlinearities have the ability to cause some sort of initial

conditions in the atmosphere (for example the weather conditions at a particular time) to rapidly escalate into completely different weather conditions. This chaotic behaviour of the atmosphere is the reason weather forecasts are not always correct, particularly forecasts made more than a few days in advance. Also the weather behaves differently to computer simulations made, due to seemingly small differences in the values in the simulation to those in reality, due to, for example, rounding the results of a numerical computation in the simulation, even to many significant figures.

This is in fact what Edward Lorenz [8] found when he was doing a computer simulation of weather at the Massachusetts Institute of Technology in the early 1960s. He wanted to repeat a run of his simulation and instead of beginning at the beginning of his run, began somewhere in the middle. He entered a series of inputs into his program that corresponded to a sequence of consecutive outputs from his previous run. What he failed to realise was that while the computer was printing out the numbers to three significant figures, it was in fact calculating the data to six. This meant that the numbers he entered in the second run were similar, but not identical, to the output of the first run.

He found that at the beginning of his run, the output of the second run closely matched the output of the first run. He went away for a while and came back to find that the program was behaving completely differently to what the previous run had indicated. The program had demonstrated one of the major properties exhibited by chaotic systems - a small change in initial conditions can, over time, result in a significant change in the state of the system. This is a property exhibited by weather patterns.

Lorenz, who was a mathematical meteorologist, provided a meteorological interpretation of this chaotic phenomenon in his 1972 talk entitled “Does the

Flap of a Butterfly's Wings in Brazil Set Off A Tornado in Texas?" [8]. This concept became known as "The Butterfly Effect", an idea that something as seemingly insignificant as the flap of a butterfly's wings can change the state of the atmosphere only minutely initially, but the air current generated by the butterfly's wings can, over a period of weeks, escalate into a major wind event, possibly even a tornado, even somewhere thousands of kilometres from the position of the butterfly.

Of course, there is no way of tracing the tornado back to a single butterfly somewhere else in the world, but it does demonstrate the sensitivity of the atmosphere.

2.2 The Equation of State: Dry Air and Wet Air

The remainder of this chapter follows chapter three of the book 'Atmosphere-Ocean Dynamics', by Adrian E. Gill [3].

The atmosphere is the body of air surrounding the Earth. Dry air is made up predominantly of the elements nitrogen, oxygen and argon, concentrated uniformly around the globe.

However the atmosphere holds water vapour, the concentration of which can vary significantly. The concentration of water is known as the specific humidity, q, defined as the ratio of the mass of water vapour to the mass of air. Since the composition of dry air does not change, it is only necessary to use q to describe the state of the air.

It is necessary to define the equation of state of the atmosphere. Air approximately obeys the ideal gas law, particularly at low pressures, which means

that air can be accurately approximated by the ideal gas law. If we allow ρ_d and p_d to represent the density and the pressure of dry air respectively (i.e. $q = 0$, no water vapour in the atmosphere), then the ideal gas law for dry air yields the equation

$$p_d = \rho_d R T \tag{2.6}$$

where T is the absolute temperature (in Kelvin), R is given by

$$R = \frac{R'}{m_a} \tag{2.7}$$

which is the universal gas constant divided by the molecular mass of dry air. The molecular mass of dry air can be easily calculated knowing the relative concentrations of the three aforementioned constituent elements, and has the value $m_a = 28.966$. This results in $R = 287.04$ J kg^{-1} K^{-1}.

However dry air only provides part of the story. We must consider the water vapour in the air, which is done in a similar way, also by applying the ideal gas law.

If e is the water-vapour pressure, ρ_v the density of the water vapour, then

$$e = \rho_v R_v T \tag{2.8}$$

where R_v is the universal gas constant divided by the molecular mass of water $m_w = 18.016$, and therefore $R_v = 461.50$ J kg^{-1} K^{-1}

The pressure of air will be the partial pressure of dry air plus the partial pressure of water vapour, meaning the total pressure is

$$p = p_d + e \tag{2.9}$$

We can substitute in the values of p_d and e from Equation 2.6 and Equation 2.8 to obtain

$$p = \rho_d R T + \rho_v R_v T \tag{2.10}$$

From the definition of the specific humidity q

$$\rho_v = q\rho \tag{2.11}$$

and also noting that the density of the mixture of water vapour and dry air is the sum of the individual densities

$$\rho = \rho_d + \rho_v \tag{2.12}$$

Defining ϵ by the equation

$$\epsilon = \frac{R}{R_v} \approxeq 0.622 \tag{2.13}$$

it is possible to write Equation 2.10 as

$$p = \rho RT(1 - q + \frac{q}{\epsilon}) \tag{2.14}$$

which is the equation of state for the atmosphere.

Typical values for q are in the range 0.004 and 0.018. We see that the partial pressure of water vapour does not make a significant difference to the total pressure.

2.3 Heat Capacity of the Atmosphere

From thermodynamics, the specific heat of a substance at constant pressure, which is denoted c_p, has a value dependent on the molecular structure of the gas in consideration. The main constituents of dry air, nitrogen and oxygen, are diatomic molecules, which have a specific heat of

$$c_p = \frac{7}{2}R \tag{2.15}$$

This is true for 99% of the composition of dry air. The composition of the remainder can be safely ignored. And the fraction of dry air in the atmosphere is $1 - q$, leading to a contribution of

$$c_{p,dry} = (1 - q)\frac{7}{2}R \tag{2.16}$$

However, water vapour, H_2O, is a triatomic molecule. So for the case of water, the specific heat is

$$c_p = 4R_v \tag{2.17}$$

and the fraction of water in the atmosphere is q, by definition of the specific humidity, resulting in

$$c_{p,vap} = 4qR_v \tag{2.18}$$

and therefore the overall specific heat of the atmosphere is

$$c_p = c_{p,dry} + c_{p,vap} = (1-q)\frac{7}{2}R + 4qR_v \tag{2.19}$$

and a little bit of simplification, using the values of R and R_v results in an atmospheric specific heat of

$$c_p = 1004.6(1 + 0.8375q) \tag{2.20}$$

with units of J kg^{-1} K^{-1}.

2.4 Stability

2.4.1 Nonsaturated Atmosphere

Overall, the density of an element of atmosphere depends on its height above the surface of the earth, usually decreasing as the height increases. This allows a static fluid to be in equilibrium, and since lighter air is on top of heavier air and not the other way round, this is a generally stable equilibrium.

But the atmosphere is a dynamic system, not a static one. Elements of the atmosphere are constantly being displaced, to consider the stability of the atmosphere accurately it is essential to account for these displacements. But to do so, we need to consider how these displacements result in changes of

properties of this element.

Before we consider an adiabatic displacement (where no energy is transferred between the atmospheric element of interest and its surroundings), we need to define several physical quantities.

The *thermal expansion rate* for the atmosphere in the ideal gas regime is given by

$$\alpha = T^{-1}, \tag{2.21}$$

which is a valid approximation to the true atmosphere, deviating by less than three parts per thousand from ideal behaviour.

Also requiring a definition is the *adiabatic lapse rate*, given in the case of an ideal atmosphere by

$$\Gamma = \frac{g}{c_p}. \tag{2.22}$$

This is the acceleration due to gravity divided by the specific heat at constant pressure.

It turns out that in all but some atmospheric conditions in the tropics, a condition for stability is

$$\frac{dT}{dz} + \Gamma > 0, \tag{2.23}$$

where z is the height above the surface of the earth.

Defining β by

$$\beta = \rho^{-1} \left(\frac{\partial \rho}{\partial q} \right)_{p,T} \tag{2.24}$$

where the subscripts p and T indicate constant temperature and pressure, it is possible to also define a variable named the buoyancy frequency, which is also known as the Brunt-Väisälä frequency, N.

The quantity given by

$$N^2 = g\alpha \left(\frac{dT}{dz} + \Gamma \right) - g\beta \frac{dq}{dz} \tag{2.25}$$

indicates how stable the atmosphere is. A positive value of N^2 represents a stable atmosphere, and a negative value represents an unstable atmosphere.

If N^2 is positive then N will clearly be real, and it is in fact the frequency at which the atmospheric element of interest oscillates vertically. For $N^2 < 0$, $N = \pm i\gamma$ is imaginary, and $e^{iNt} \equiv e^{\pm\gamma t}$. One of these solutions exhibits exponential growth and is therefore unstable. The other solution decays exponentially and is therefore stable, diminishing as time passes.

2.4.2 Saturated Atmosphere

A saturated atmosphere renders the arguments of Section 2.4.1 invalid, particularly for air travelling upwards. This is due to the fact that the higher air travels, the less water vapour it is capable of carrying, with the result that some water vapour is forced to condense, which increases the buoyancy of the

atmospheric element. Since water vapour is forced into its liquid form, latent heat must be released, which in turn increases the buoyancy of the element of atmosphere that is of interest.

A different lapse rate, the *pseudoadiabatic lapse rate* denoted Γ_s, is used in this case, and the term 'pseudoadiabatic' is used because as material is being lost it is not quite adiabatic. This lapse rate is calculated assuming the liquid water resulting from the condensation becomes precipitation as it is removed, with the result that the buoyancy of the atmospheric element of interest is unaffected.

Calculation of Γ_s is done by assuming the mass of dry air in the element remains unchanged while the amount of water vapour contained inside it changes. Defining the mixing ratio to be the mass of water vapour to the mass of dry air, i.e.

$$r = \frac{q}{(1-q)} \tag{2.26}$$

Then the changes in vapour concentration must obey

$$\frac{dr}{(1+r)} = \frac{dq}{(1-q)} \tag{2.27}$$

As we are considering a pseudoadiabatic case, Equation 2.27 gives the ratio of condensed water mass to moist air mass, and as the air parcel of interest is saturated, then q and r take the values q_w and r_w respectively. If L_v is the latent heat released by water vapour, then the change in heat content is given

by L_v times Equation 2.27. If T is absolute temperature and q_w the value of specific humidity corresponding to saturation, then the equation of entropy is

$$L_v \frac{dq_w}{1-q_w} + c_p dT - T \left(\frac{\partial v_s}{\partial T} \right)_p dp = 0 \tag{2.28}$$

Also, the differential of q_w can be written

$$dq_w = \left(\frac{\partial q_w}{\partial T} \right)_p dT + \left(\frac{\partial q_w}{\partial p} \right)_T dp \tag{2.29}$$

Substituting this, and the hydrostatic equation

$$dT = -\Gamma dz \tag{2.30}$$

and an alternative definition for α, namely

$$\alpha = -\rho^{-1} \left(\frac{\partial \rho}{\partial T} \right)_p \tag{2.31}$$

results in

$$\Gamma_s \left(1 + \frac{L_v}{c_p(1-q_w)} \left(\frac{\partial q_w}{\partial T} \right)_p \right) = \Gamma \left(1 - \frac{\rho L_v}{\alpha T(1-q_w)} \left(\frac{\partial q_w}{\partial p} \right)_T \right) \tag{2.32}$$

The value of the pseudoadiabatic lapse rate (in units of K km^{-1}) is given approximately by the equation

$$\Gamma_s = 6.4 - 0.12t + 2.5 \times 10^{-5}t^3 + [10^{-3}(t-5)^2 - 2.4](1 - \frac{p}{p_r}) \qquad (2.33)$$

where t is the temperature in degrees Celsius, p the pressure in mb and $p_r = 1000$ mb. For temperatures of $-40 < t < 40$ and pressures of $500 < p < 1000$, this equation is accurate to within 0.2 K km^{-1}. However it is important to note that the air pressure in the atmosphere frequently exceeds 1000 mb, so this approximation is at its most useful in regions of low pressure.

The latent heat of vapourisation L_v is also a quantity that depends on temperature, and its value in J kg^{-1} is given by

$$L_v = 2.5008 \times 10^6 - 2.3 \times 10^3 t \qquad (2.34)$$

2.5 Vorticity and Circulation

In both fluid dynamics and meteorology, the quantity defined by

$$\boldsymbol{\omega} = \nabla \times \mathbf{v} \qquad (2.35)$$

is very significant. It describes the rotation of the fluid. As a fluid flows, it flows in either a purely translational manner, or there is a rotational component to its motion. In the former case, the vorticity will have a value of zero (and the fluid termed *irrotational*), but in the presence of a rotational component, the vorticity will have a nonzero value where the sign indicates whether the fluid is rotating clockwise or anticlockwise, whereas the magnitude indicates the speed of rotation.

In the idealised situation where the fluid of interest flows without turbulence, the vorticity will be zero except at the periphery of the volume occupied by the fluid. However, in most real world fluids, turbulence does exist, meaning that while the fluid is travelling in a particular direction in a global sense, locally, there will be some locations in which individual fluid elements are travelling in other directions. This means that in general the vorticity of the fluid will be nonzero everywhere, although there may be particular points within the fluid where the vorticity does instantaneously have a value of zero.

Meteorologists use vorticity in a similar way. They are often interested in the rotation of infinitesimal parcels of air about a vertical axis. In meteorology, air that spins in a cyclonic direction (anticlockwise, in the northern hemisphere, when viewed from space, and in the opposite direction for the southern hemisphere) is defined to possess positive vorticity whereas air that undergoes anticyclonic rotation is defined to possess negative vorticity.

Meteorologists are interested in vorticity from two sources [1]. One is known as planetary vorticity, which is rotation imparted on the parcels of air due to the rotation of the Earth. Everywhere but at the equator, the rotation of the earth imparts a rotation of the air about a local vertical axis, and the magnitude of rotation experienced by the air parcels is proportional to the sine of the local latitude - maximal at the poles and minimal at the equator.

There is another source of vorticity that is not related to the motion of the Earth. This is known as relative vorticity, and is partially the result of the natural turbulence of the air, but is also partially induced by the air navigating the curved surface of the Earth's surface (which would result in some north-south motion as well as east-west motion even if the Earth was stationary, due to the east-west distance around the Equator being larger than the east-west distance around the rest of the planet. But, the east-west velocity of

the air about the Earth is not the same at all longitudes; it will vary slightly with longitude, due to mountains, and other obstacles as the Earth is not a perfect sphere. This results in a horizontal shear that also induces north-south velocity resulting in some rotation and hence affecting the relative vorticity.

Naturally enough, the sum of the relative vorticity and the planetary vorticity gives the total vorticity experienced by an atmospheric parcel. This total vorticity is called the absolute vorticity.

In a fluid dynamics context, it can be shown that in the case of a fluid rotating uniformly (as though a solid body would), the vorticity has a value of precisely double the angular velocity. We will now show this, using a proof similar to that found in [5]..

Consider the three points on one of the $z = const$ faces of a three dimensional rectangular element of fluid (depicted in Fig 2.1). At each of the three points the fluid flows in the plane such that at each of the points there is an x-component of the fluid velocity and a y-component. The six velocities can be written in differential form, as

$$V_{x,A} = V_x \tag{2.36}$$

$$V_{y,A} = V_y \tag{2.37}$$

$$V_{x,B} = V_x + \frac{\partial V_x}{\partial x} dx \tag{2.38}$$

$$V_{y,B} = V_y + \frac{\partial V_y}{\partial x} dx \tag{2.39}$$

$$V_{x,C} = V_x + \frac{\partial V_x}{\partial y} dy \tag{2.40}$$

$$V_{y,C} = V_y + \frac{\partial V_y}{\partial y} dy \tag{2.41}$$

$$\tag{2.42}$$

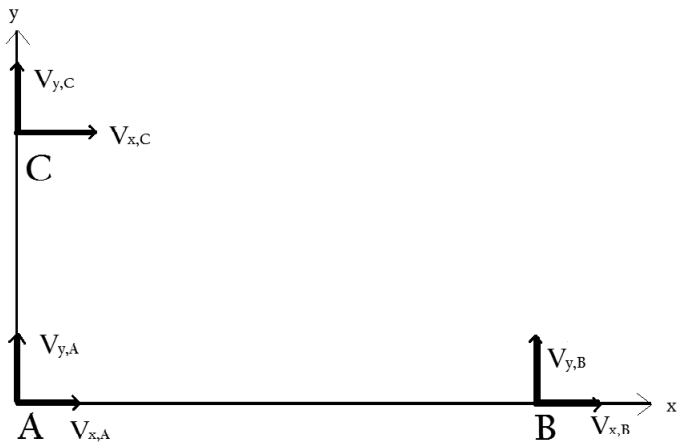

Figure 2.1: One of the faces of a cuboid shaped element of fluid parallel to the $x-y$ plane. On this diagram are three points, A, B and C, and at each of those three points, there exists an x-component and a y-component of the velocity field.

As this face is infinitesimally small, the angular velocity about the z-axis is given by the average of the difference between the y-component of the velocities at points A and B, and the difference between the x-component of the velocities at points A and C, i.e.

$$\Omega_z = \frac{1}{2}\left(\frac{V_{y,B} - V_{y,A}}{dx} - \frac{V_{x,C} - V_{x,A}}{dy} \right) \tag{2.43}$$

where the second term is negative since we are considering anticlockwise motion about the z-axis, meaning fluid flows from C to A (i.e. travels along the y-axis in the negative direction), and then from A to B (i.e. travels along the x-axis in the positive direction). Substituting the differential form of $V_{y,B}$ etc. results in

$$\Omega_z = \frac{1}{2}\left(\frac{V_y + \frac{\partial V_y}{\partial x}dx - V_y}{dx} - \frac{V_x + \frac{\partial V_x}{\partial y}dy - V_x}{dy} \right) \tag{2.44}$$

or, more simply,

$$\Omega_z = \frac{1}{2}\left(\frac{\frac{\partial V_y}{\partial x}dx}{dx} - \frac{\frac{\partial V_x}{\partial y}dy}{dy} \right) \tag{2.45}$$

which can be written

$$\Omega_z = \frac{1}{2}\left(\frac{\partial V_y}{\partial x} - \frac{\partial V_x}{\partial y} \right) \tag{2.46}$$

which is exactly half the z-component of the vorticity, ω_z. A similar proof in the $x - z$ plane shows

$$\Omega_y = \frac{1}{2}\left(\frac{\partial V_x}{\partial z} - \frac{\partial V_z}{\partial x} \right) = \frac{\omega_y}{2} \tag{2.47}$$

and in the $y - z$ plane it can be shown

$$\Omega_x = \frac{1}{2}\left(\frac{\partial V_z}{\partial y} - \frac{\partial V_y}{\partial z} \right) = \frac{\omega_x}{2} \tag{2.48}$$

and hence, the angular velocity is half of the vorticity.

Returning to the notion of absolute vorticity, we can now find an expression for the absolute vorticity of a fluid particle involving the angular velocity of the rotating body, which in meteorology, is Earth. Let $\boldsymbol{\omega_r}$ be the relative vorticity. The planetary vorticity is given by $2\boldsymbol{\Omega}$ so that the absolute vorticity can be written

$$\boldsymbol{\omega} = \boldsymbol{\omega_r} + 2\boldsymbol{\Omega} \tag{2.49}$$

2.6 Circulation

Circulation is a quantity directly related to the vorticity. A vortex line is defined to be an imaginary line in the fluid, which is everywhere tangential to the vorticity vector along that line. In the case of Earth, the vortex lines due to planetary vorticity are lines parallel to the axis of the Earth.

It is possible to define a vortex "tube", a three dimensional structure in which the ends are closed curves, and the sides composed of vortex lines (In the case of the closed curves being circular, a vortex tube is a cylinder that may or may not be bent). By definition, on the surface of such a vorticity tube, vorticity vectors run tangentially, meaning that the value of the vorticity inside the tube can not change as vorticity vectors do not cross the surface, no vorticity can enter or leave the tube. As the divergence of the curl of any vector vanishes, vorticity has zero divergence and therefore the volume integral of the divergence of the vorticity must also vanish, i.e.

$$\int_V \nabla \cdot \boldsymbol{\omega} dV = 0 \tag{2.50}$$

The divergence theorem permits us to write this as

$$\int_A \boldsymbol{\omega} \cdot \hat{\mathbf{n}} dA = 0 \tag{2.51}$$

where we have introduced $\hat{\mathbf{n}}$ to be the outward pointing vector of the ends of the tube (noting that the integrand is identically zero on the remainder of the

surface as the vorticity is perpendicular to the outward pointing normal).

If we allow the surface area of the two ends of the tube to be A and A' respectively, then the implication is that

$$\int_A \boldsymbol{\omega} \cdot \hat{\mathbf{n}}_A dA + \int_{A'} \boldsymbol{\omega} \cdot (-\hat{\mathbf{n}}_A) dA' = 0 \tag{2.52}$$

where the sign of $\hat{\mathbf{n}}_{A'}$ is negative because the fluid is travelling along the tube. It enters the tube through area A' and exits through area A. It is therefore travelling in the opposite direction to $\hat{\mathbf{n}}_{A'}$.

Equation 2.52 implies that

$$\int_A \boldsymbol{\omega} \cdot \hat{\mathbf{n}}_A dA = -\int_{A'} \boldsymbol{\omega} \cdot \hat{\mathbf{n}}_{A'} dA' \tag{2.53}$$

where now the orientation of $\hat{\mathbf{n}}_A$ and $\hat{\mathbf{n}}_{A'}$ are pointing in the same direction if we straighten out the vortex tube to be a cylinder. This means the outward flux at the A end of the tube is equal to the inward flux at the A' end, and either one of these fluxes can be labelled the strength, i.e.

$$\Gamma = \int \boldsymbol{\omega} \cdot \hat{\mathbf{n}} dA \tag{2.54}$$

If we do so we can see from Equation 2.53 that the strength of the vortex tube must be the same at both ends of the tube. But the tube is arbitrarily long - we can take our old vortex tube and cut it into two smaller tubes, making the cut at an arbitrary location along its length. We must end up with

two tubes, for each of which both ends of the tube must have the same vortex strength. This argument implies that the strength of a vortex tube must be uniform along its length.

Stokes' Theorem tells us we can also write the vortex tube strength in terms of a closed curve integral, with

$$\Gamma = \oint_C \mathbf{v} \cdot d\mathbf{r} \tag{2.55}$$

where the line integral of $\mathbf{v}$ around the curve in question is known as the circulation. The circulation is therefore another quantity which can describe Γ, and the vorticity. However, the vorticity is a vector while the circulation is a scalar.

It can be shown (Pedlosky, page 29) [10], that the rate of change of the circulation is given by

$$\frac{d\Gamma}{dt} = \oint_c \frac{d\mathbf{v}}{dt} \cdot d\mathbf{r} \tag{2.56}$$

In the case of a uniformly rotating fluid subject to a Coriolis force (which we will later see is $2\boldsymbol{\Omega} \times \boldsymbol{u}$ where $\boldsymbol{\Omega}$ is the angular velocity of the rotation, the momentum equation becomes

$$\frac{D\mathbf{v}}{Dt} = -\frac{\nabla \mathbf{p} + 2\boldsymbol{\Omega} \times \mathbf{v} + \mathbf{F}}{\rho} \tag{2.57}$$

and so the rate of change of the circulation is given by a sum of three terms, each denoting one way of changing the circulation and therefore the strength of the vortex. The first is by changing the pressure gradient force, the second is by changing the angular velocity (although this is constant in the case of the

Earth's motion) and the third is by changing any other forces the fluid may be experiencing (such as gravity).

2.7 Enstrophy

There is a further quantity that needs to be defined, for it will be used later. This quantity is known as the fluid's enstrophy, and is given by

$$\epsilon = \frac{1}{2}\int \omega^2 dV \tag{2.58}$$

where

$$\omega^2 = \boldsymbol{\omega} \cdot \boldsymbol{\omega} \tag{2.59}$$

The enstrophy is a measure related to the turbulence of the fluid. Taking the dot product with the Navier-Stokes equation (Equation 2.5), and integrating over the volume (noting that integrating the nonlinear terms in the Navier-Stokes equation yields zero, to leave

$$\frac{1}{2}\frac{d}{dt}\int \rho v^2 dV = -\frac{1}{2}\nu \int \rho \omega^2 dV \tag{2.60}$$

It has also been said to act as a dissipation coefficient - that is, to describe how effective the fluid is at dissipating energy. The left hand side is the time derivative of the kinetic energy of the fluid, and therefore the total enstrophy of the fluid is equal to time derivative of the kinetic energy divided by $-\nu$ where ν is the viscosity of the fluid.

2.8 Dimensions

In this section we will determine the dimensions of the vorticity, circulation and enstrophy. For the purposes of the Rossby Wave simulations discussed later, in which enstrophy is a very important quantity, it is desirable to know the dimensions of this particular quantity.

2.8.1 Vorticity

Vorticity is as defined in Eq 2.35. A componentwise definition of the vorticity readily follows from the Eqs 2.46-2.48. From this, we can easily see that the vorticity must have the dimensions of $\frac{\partial \mathbf{v}}{\partial x}$. As $\mathbf{v}$ is a velocity, it must have dimensions of $[L][T^{-1}]$, a length times an inverse time. Now x is a length, so it follows that the vorticity has dimensions $[T^{-1}]$, an inverse time. This is consistent with the previously derived theorem relating the vorticity and the angular velocity, in the case of a fluid undergoing uniform rotation - we know that angular velocity also carries the dimensions of inverse time.

2.8.2 Circulation

The circulation is as defined by Eq 2.56. Hence, it is clear that the circulation must carry the dimensions of $\mathbf{v} \cdot d\mathbf{r}$, which must be a velocity times a length, so it has dimensions $[L^2][T^{-1}]$.

2.8.3 Enstrophy

Enstrophy is as defined by Eq 2.58. We already know the dimensions for vorticity. It follows from Eq 2.58 that the dimensions of the enstrophy are $[L^3][T^{-2}]$. This is dimensionally consistent with energy per unit mass.

Chapter 3

The Beta Plane and Rossby Waves

3.1 Coriolis Acceleration

The Earth is approximately a sphere, rotating about an axis 23° from the vertical in a west-to-east direction. The Earth is a rotating frame of reference and is thus subject to a Coriolis force.

Let $\mathbf{\Omega}$ denote the angular velocity at which the Earth rotates. Noting that the Earth completes one full rotation per sidereal day, and that one day is not quite 24 hours, but 23 hours, 56 minutes and 4 seconds. This is equal to 86164 seconds, the angular velocity of the Earth in radians per second is

$$\frac{2\pi}{86164} \approxeq 7.2921 \times 10^{-5} \tag{3.1}$$

If $\mathbf{x}_r$ is used to represent a fixed position on the rotating frame, this fixed position has a velocity of $\mathbf{\Omega} \times \mathbf{x}_r$. As a consequence, the velocity of that point relative to the stationary frame of reference is

$$\frac{d\mathbf{x}_s}{dt} = \frac{d\mathbf{x}_r}{dt} + \mathbf{\Omega} \times \mathbf{x}_r \tag{3.2}$$

The acceleration in the stationary frame can be written

$$\frac{d^2\mathbf{x}_s}{dt^2} = \frac{d}{dt}\left(\frac{d\mathbf{x}_s}{dt}\right) \tag{3.3}$$

and substituting Equation 3.2 into Equation 3.3 tells us that the acceleration is given by

$$\frac{d\mathbf{v}_s}{dt} = \frac{d\mathbf{v}_r}{dt} + 2\mathbf{\Omega} \times \mathbf{v}_r = \mathbf{\Omega} \times (\mathbf{\Omega} \times \mathbf{x}_r) \tag{3.4}$$

introducing the notation that for the stationary reference frame $\mathbf{v}_s \equiv \frac{d\mathbf{x}_s}{dt}$ and similarly with r subscripts for the rotating frame of reference. Employing a vector identity, this can also be written

$$\frac{d\mathbf{v}_s}{dt} = \frac{d\mathbf{v}_r}{dt} + 2\mathbf{\Omega} \times \mathbf{v}_r - \frac{1}{2}\nabla(\Omega x_r)^2 \tag{3.5}$$

This is the overall acceleration. The Corolis acceleration is the middle term on the right hand side featuring the cross product. If we treat the Earth to be perfectly spherical and the rotation of the earth to be completely in the azimuthal direction, then the angular velocity of the earth, as a vector, is

$$\mathbf{\Omega} = (r, \theta, \phi) = (0, 0, 7.2921 \times 10^{-5}) \tag{3.6}$$

when using a spherical coordinate system and rad/s units.

3.2 The Coriolis Parameter

In the previous section we found the angular velocity of the earth to be 7.2921 $\times 10^{-5}$ radians per second. Closely related to this is the Corolis parameter, also known as the Coriolis frequency, which at a given location on the Earth's surface has a value given by

$$f = 2\Omega \sin \chi \tag{3.7}$$

where χ is the latitude of the location of interest. Clearly the Coriolis parameter has a value of 0 at the equator and a maximum value of $2\Omega = 1.4582 \times 10^{-4}$ rad/s at the poles. The Coriolis parameter is defined to be positive for the northern hemisphere and negative for the southern hemisphere. This sign convention is important because an atmospheric rotation which has the same sign (the sign of the rotation signifies its direction) as the Coriolis parameter is called *cyclonic* whereas a rotation in the opposite direction to the Coriolis parameter is called *anticyclonic*.

A commonly used approximation in geophysics is the f-plane appromimation. It assumes a uniform value of χ, and therefore of f. This is applicable when considering an area covered by only a very small change in latitude.

3.3 Beta Plane Approximation

A better approximation of the value of f is the beta approximation. This assumes that the value of f does not remain uniform, but varies linearly with latitude, assuming a form

$$f = f_0 + \beta y \tag{3.8}$$

where f_0 is some reference Coriolis parameter at a particular latitude, y is a distance from the equator and β is a variable describing how rapidly the Coriolis parameter changes with latitude. This approximation is obtained by performing a Taylor expansion on the definition of the Corolis Parameter, Equation 3.7. It turns out that β is called the Rossby parameter and has a value given by

$$\beta = 2\frac{\Omega cos\chi}{a} \tag{3.9}$$

where a is the radius of the Earth.

3.4 Mid Latitude Beta-Plane Approximation

With the northernmost part of New Zealand, Tom Bowling Bay, being at a latitude of 34.4° S and the southernmost part of Stewart Island at a latitude of 47.3° S, the mid-latitute Beta-Plane approximation is valid for New Zealand.

With this latitude range, the Coriolis Parameter ranges between 8.2383 $\times$ 10^{-5} and 1.0717 $\times$ 10^{-4}, a variation of just less than 20%. The Coriolis parameter does not have a uniform value throughout NZ so the f-plane approximation is not valid. It is better to use the β-plane approximation. Also, at the equator, the Rossby parameter vanishes due to the latitude being zero. Here the β-plane approximation is equal to the f-plane approximation. At the equator, the Rossby parameter takes on its maximum value of $\beta = 2\frac{\Omega}{a}$, while it has a value of zero at the poles.

3.5 Rossby Radius of Deformation

The main horizontal (in other words, applying to the x- and y- coordinates only) lengthscale relating to Rossby Waves is known as the Rossby Radius of Deformation. It is the horizontal scale at which the Coriolis force begins becoming significant. Contrary to popular belief, the swirling of water as it goes through a plughole down the drain is in no way affected by the Coriolis force - a sink or a bathtub has a length which is typically much smaller (usually several orders of magnitude smaller) than the Rossby Radius of Deformation. For the atmosphere, it has a value typically in the order of about 10^5 to 10^6 metres, but it can vary considerably. It does depend on latitude, as it is given by the formula

$$L_R = \frac{c_g}{f} \tag{3.10}$$

Note that this equation implies the Rossby Radius of Deformation increases as one approaches the equator, and in fact becomes undefined at the equator. This is to be expected, as the Coriolis force acts to deflect fluid away from the equator in order to induce rotation in the fluid. The Coriolis force therefore will not act on a fluid at the equator. So no matter how large the horizontal lengthscale of a fluid at the equator is (particularly in the x-direction), it will never be large enough for Coriolis effects to become significant. Of course, if it is a large body of fluid that one is interested in, it will occupy a significant range in the y-direction too, and the Coriolis force will push both the northern edge and the southern edge away from the equator, stretching the body of fluid in the meridonial direction.

Chapter 4

Atmospheric Rossby Waves

Rossby waves were named after Carl-Gustac Rossby who first theorised their existence in 1939, in his paper "Relation between variations in the intensity of the zonal circulation of the atmosphere and the displacements of the semi-permanent centres of action" [11].

Rossby waves can only form if the Rossby parameter does not vanish, $\beta \neq 0$. Rossby waves form at the equator and in both hemispheres but cannot form at the poles due to β having a local value of 0 there.

Rossby waves are slow-moving waves, with a very long wavelength which generally travel in an east to west direction. They exist because of the shear forces on the atmosphere resulting from the variation of the Coriolis force experienced by the atmosphere as a function of latitude. In a hypothetical cylindrical planet, the Coriolis force would not vary with latitude on the curved surface and therefore Rossby waves would not form. Rossby waves are an artifact of the spherical shape of the Earth.

4.1 Derivation of Dispersion Relation of Rossby Waves in a Barotropic Atmosphere

We will now derive a dispersion relation for the two dimensional (horizontal only) motion of Rossby waves, under the assumption that the atmosphere is a barotropic substance (in which the pressure is a function of density only) and let us assume these two quantities are constant. This derivation applies to a barotropic atmosphere, which is an atmosphere that assumes the pressure is dependent only on the density, in other words

$$p = p(\rho) \tag{4.1}$$

It is important to make this assumption so that we can idealise the nature of the atmosphere - in reality it is too chaotic to model accurately without making such an idealisation. However we are considering waves travelling through a large body of air, and as the air does not have uniform density everywhere, but rather decreases as altitude increases, which prevents us from using an assumption that the atmosphere is incompressible.

Since Rossby waves are indeed waves, let us use a wavelike stream function in this derivation, Let x be the coordinate direction parallel to the equator (i.e. west-east, which is also known as the *zonal* coordinate and y be the coordinate direction from pole to pole (i.e. north-south, which is also known as the *meridonial* coordinate). Our stream function is

$$\psi = Ae^{i(kx+ly-\omega t)} \tag{4.2}$$

Assume the flow is entirely parallel to the equator with uniform speed U, with zero vorticity. Let us perturb this flow, so the component of the flow parallel

to the equator is

$$u = U + u'(x, y, t) \tag{4.3}$$

and the poleward component of the flow

$$v = 0 + v'(x, y, t) = v'(x, y, t) \tag{4.4}$$

This is to be a small perturbation only: $U \gg u', U \gg v'$. Also, using our stream function

$$u = \frac{\partial \psi}{\partial y} \tag{4.5}$$

$$v = -\frac{\partial \psi}{\partial x} \tag{4.6}$$

and the relative vorticity can be written in the form

$$\eta = \nabla^2 \psi \tag{4.7}$$

and substituting in the value of our stream function and simplifying we find

$$\eta = -(l^2 + k^2)\psi \tag{4.8}$$

If there is no advection of relative vorticity present, then it must be that

$$\frac{d(\eta + f)}{dt} = 0 \tag{4.9}$$

This equation is a statement of the law that vorticity must be conserved, which is a direct consequence of the conservation of angular momentum. Writing this

last equation out in full applying the chain rule from calculus

$$\frac{\partial \eta}{\partial t} + \frac{\partial \eta}{\partial x}\frac{dx}{dt} + \frac{\partial \eta}{\partial y}\frac{dy}{dt} + \frac{\partial f}{\partial y}\frac{dy}{dt} = 0 \tag{4.10}$$

By definition

$$U + u' \equiv \frac{dx}{dt} \tag{4.11}$$

$$\beta \equiv \frac{\partial f}{\partial y} \tag{4.12}$$

$$v' \equiv \frac{dy}{dt} \tag{4.13}$$

And since $\frac{dy}{dt}$ is small, the third term on the left hand side is negligible. The perturbation is used only for the term involving the Coriolis parameter, for the terms involving the relative vorticity, the approximate constant flow solution $u \approx U, v \approx 0$ is employed.

We are therefore left with the equation

$$0 = \frac{\partial \eta}{\partial t} + U\frac{\partial \eta}{\partial x} + \beta v' \tag{4.14}$$

and substituting in the values of η and v' and multiplying through by -1 yields

$$0 = (l^2 + k^2)\frac{\partial \psi}{\partial t} + (l^2 + k^2)U\frac{\partial \psi}{\partial x} + \beta\frac{\partial \psi}{\partial x} \tag{4.15}$$

Noting that

$$\frac{\partial \psi}{\partial x} \equiv ik\psi \tag{4.16}$$

$$\frac{\partial \psi}{\partial t} \equiv -i\omega\psi \tag{4.17}$$

this can be written

$$i\omega(l^2+k^2)\psi = Uik(l^2+k^2)\psi + \beta ki\psi \tag{4.18}$$

and dividing through by $i\psi(l^2+k^2)$ results in a dispersion relation of

$$\omega = k(U + \frac{\beta}{l^2+k^2}) \tag{4.19}$$

From this dispersion relation, the phase speed and the group speed can be calculated. The zonal component of the phase speed of the waves is given by

$$c \equiv \frac{\omega}{k} = U + \frac{\beta}{l^2+k^2} \tag{4.20}$$

whereas the meridonial component is given by

$$\frac{\omega}{l} = \frac{k}{l}(U + \frac{\beta}{l^2+k^2}). \tag{4.21}$$

The zonal component of the group speed is given by

$$\omega = U + \frac{\beta(l^2-k^2)}{(l^2+k^2)^2} \tag{4.22}$$

and the meridonial component is just

$$\frac{\partial\omega}{\partial l} = -\frac{2\beta l}{l^2+k^2} \tag{4.23}$$

Note that if $l = k$, then the group speed is just U, and if the Rossby parameter β is equal to zero, there will also be no Rossby waves, and both the group speed and phase speed are equal to U, in the zonal direction only .

The Rossby Wave owes its existance to the presence of an vorticity gradient. As we saw in Chapter 2, the vorticity increases in magnitude with latitude, and Rossby Waves are the atmosphere's response to this planetary vorticity gradient. But how does a change in vorticity result in a waveform? We will need to consider three fluid columns on a line of constant latitude around the Earth. But before we do so, it is necessary to define a quantity known as "potential vorticity".

This potential vorticity is given by

$$\Pi = \frac{\omega + 2\Omega}{\rho} \cdot \nabla\lambda \tag{4.24}$$

where λ represents some scalar property of the fluid, such as pressure, temperature or density. If the fluid motion is adiabatic, the quantity λ is conserved, but this is not necessary as long as its rate of change can be exactly determined.

Also let ζ be the vertical component of the vorticity, ω_z.

Consider three columns of fluid, C_1, C_2 and C_3. Allow them to traverse the lines of constant latitude, so they are initially travelling in the x-direction only. Then displace C_2 away from the equator, so that it is subject to greater planetary vorticity. But the "wave" potential vorticity, which is given by $\zeta_0 - F\eta_0$, where F is a lengthscale parameter, must compensate for this increase in potential voricity of C_2, to conserve the total potential vorticity of the sustem. The result of this is that C_2 experiences some vortex tube compression, and as the atmosphere is not solidly bounded above, this has the effect of stretching the vortex tube. This reduces the relative vorticity of C_2 in the presence of planetary vorticity. It will also have a greater wave amplitude than both of the as yet undeviated columns, increasing its value of η_0. This

induces a change in circulation by the concentrated region of negative relative vorticity about C_2, as well as the increase in the value of η_0 inducing an increase in pressure locally around C_2. These two effects reinforce each other to deflect the two neighbouring columns C_1 and C_3 away from the line of constant latitude. It would cause C_1 to increase in latitude while C_3 decreases in latitude. So now the first two columns are at about the same latitude while C_3 is at a much lower latitude than the others, it has a lower relative potential vorticity, and as a result, the "wave" potential vorticity must compensate to keep the potential vorticity of the system of three particles unchanged. The same process repeats with C_3 being the centre of the rotation (instead of C_2 as was previously the case). The rotation occurs in the opposite direction, since the potential vorticity had to increase, not decrease, this time in order to compensate. So this results in a rotation forcing C_2 back towards, and in fact past, the original line of constant latitude. (The inertia of C_2 causes it to overshoot). This is a microscopic view of the oscillation that occurs to induce a Rossby Wave on a macroscopic scale.

4.2 Resonant Rossby Wave Triads

Rossby Wave triads consist of three Rossby Waves that interact with each other in a manner such that the superposition of the first two waves drives the other wave. They do interact in a nonlinear fashion, but the nonlinear interactions of the three constituent waves only exchange energy, without producing additional waves. It is the linear interaction of the waves that gives rise to the creation of the waves.

A Rossby Triad solution must be the sum of three individual Rossby Waves. That is, it must have the form

$$\psi = \Sigma_{n=1}^{3} \Re(a_n \exp[i(k_n x + l_n y - \sigma_n t)]) \tag{4.25}$$

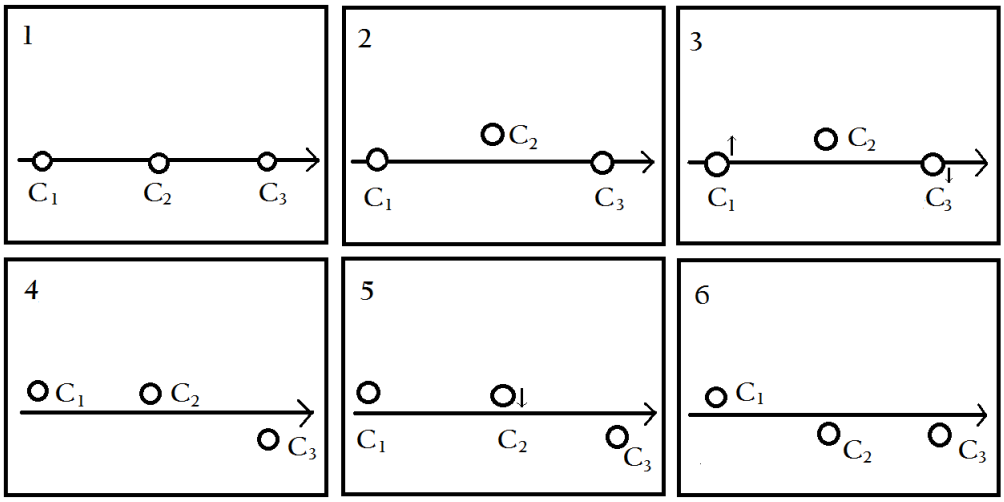

Figure 4.1: A bird's eye view of three columns of fluid on a line of constant latitude (1). The middle column, C_2, gets displaced away from the equator, resulting in an increased latitude (2).In order to conserve potential vorticity in the system, the other two columns of fluid have to leave the original line of constant latitude (3). C_1 increases in latitude whereas C_3 decreases in latitude (4). Now columns C_1 and C_2 are at approximately the same latitude whereas C_3 is at a completely different latitude. As before the system acts to conserve potential vorticity, causing C_2 to decrease in latitude (5). Now C_2 and C_3 have a similar latitude, and conservation of potential vorticity results in a force on C_1, causing it to decrease in latitude also (6).

Assuming the amplitudes, wavenumbers and frequencies are all purely real, this reduces, using Euler's Identity, to

$$\psi = \Sigma_{n=1}^{3} a_n \cos(k_n x + l_n y - \sigma_n t) \tag{4.26}$$

It can be shown [9] that in order for a triad of Rossby Waves to resonate in the required manner, the wavenumbers and frequencies must obey the following relationships:

$$k_1 \pm k_2 \pm k_3 = 0 \tag{4.27}$$

$$l_1 \pm l_2 \pm l_3 = 0 \tag{4.28}$$

$$\sigma_1 \pm \sigma_2 \pm \sigma_3 = 0 \tag{4.29}$$

In a Rossby Triad, the potential vorticity is conserved, which means the Rossby Triad must satisfy the differential equation

$$\frac{\partial}{\partial t}[\nabla^2\psi - F\psi] + \left(\frac{\partial\psi}{\partial x}\frac{\partial\nabla^2\psi}{\partial y} - \frac{\partial\psi}{\partial y}\frac{\partial\nabla^2\psi}{\partial x} \right) + \beta\frac{\partial\psi}{\partial x} = 0 \tag{4.30}$$

where $F = \frac{1}{L_R^2}$ is the reciprocal of the square of the Rossby Radius of Deformation, defined on page 33. For a Rossby wave, the second term (in parentheses, known as the Jacobian term) is identically zero. It is possible to derive a form of the dispersion relationship of such waves (in which the variable F appears) by directly substituting Equation 4.25 into the remaining terms of Equation 4.30.

Doing so for ψ_n, a single Rossby wave, which is one of the three components that makes up the triad, results in

$$-\sigma_n a_n(k_n^2+l_n^2+F)\sin(k_n x+l_n y-\sigma_n t)+\beta k_n a_n \sin(k_n x+l_n y-\sigma_n t)=0, \quad (4.31)$$

which reduces to

$$\sigma_n = \frac{\beta k_n}{k_n^2 + l_n^2 + F} \quad (4.32)$$

This equation is true when one wave component is present. However, the interaction of multiple wave components in general will give a nonzero Jacobian term. This results in a nonlinearity which creates a new wave. Suppose there are originally two wave components interacting with one another. These interact to bring about a third wave. But this new wave will in turn interact with the two preexisting wave components to produce a fourth and a fifth wave. Typically, a Rossby triad consists of a simplified look at the initial stages of this phenomenon, prior to the development of the fourth wave component. The purpose of this simplification is to focus the studying of a Rossby triad purely to the mechanism in which a new wave is created from two existing wave components. Of particular interest is a Resonant Rossby wave triad, in which, instead of the interactions of the third wave with the first and second yielding fourth and fifth waves, they act to reinforce the original two waves.

Peter Lynch, in 2001 [9], compared the dynamics of a Rossby wave triad to those of a swinging spring - essentially a pendulum in which the string is replaced with a spring which oscillates along its length. This adds an extra mode to the motion of the pendulum so that its motion is not just purely tangential as is the case for a normal pendulum, but also includes some radial oscillation. It is assumed that the mass of the spring itself is negligible in comparison to the weight at the end of the spring. One might intuitively expect

the motion of the swinging spring to be entirely predictable, but as the two modes continually exchange energy, this is not the case. This energy exchange also depends on the relative frequencies of the two oscillations - something that in practice depends slightly on the damping of the motion.

An exchange in energy between the two modes that yields a condition of resonance, has been found to take place when the oscillation of the spring has a frequency exactly double that of the swinging mode. Lynch then investigated what happened when the frequency of the spring's oscillation became much greater than the oscillation of the pendulum. He found this model to be an ideal analogy for the dynamics of the atmosphere, which also has two modes of oscillation - the high frequency oscillation resulting from gravity waves and also a lower frequency Rossby mode of oscillation. He compared the nonlinear energy exchanges between the two modes in the swinging spring system and the atmosphere, and demonstrated that such nonlinear energy exchanges in the swinging spring model resulted in a chaotic motion. This is exactly what is observed in the atmosphere.

Lynch went on to investigate the conditions under which the spring resonated, and he found that the plane of the swinging precessed. On investigation of the equations of motion of the spring, he found they were analogous to the equations of motion of a Rossby triad - the dynamics of the two systems are mathematically equivalent in the case of motion with small amplitudes (small enough to prevent the exhibition of chaos). The equation for the swinging spring was found to be analogous to the equation of energy of the Rossby triad, and similarly, the equation for the total angular momentum of the swinging spring was found to be identical to that of the enstrophy of the Rossby triad. Numerical experimentation showed a complete transfer of energy would take place - if the spring was set in motion such that almost all of its mechanical energy lay in the oscillation of the spring, over time the energy would be

lost to the swinging mode, so that it would behave like a pendulum. Then energy would be transferred back to the oscillation of the spring - and then back to the motion of the pendulum - only this time it would swing in a different direction to the first time that the energy was all in the pendulum mode. This is the precession of the swing phase.

Lynch concluded that since both systems follow mathematically equivalent governing equations, this precession of the swing phase must have an analogy in the world of Rossby Triads, even though nobody studying the dynamics of the triads without the benefit of the swinging spring analogy had observed any phenomena that would be it. It was found that the phase of the Rossby Triads also showed the same sort of precession, so while the motion happened to be all in a single direction, there was an extra, formerly hidden, mode of oscillation in the Rossby Triads system. The discovery of this extra mode of oscillation in Rossby Triads had its implications for the predictability of atmospheric behavour and therefore the weather.

It meant that even if the flow of the atmosphere consisting predominantly of a single Rossby wave of a relatively large amplitude (so that most of the energy of the flow was in this Rossby wave), such a wave could be unstable, and turbulence naturally found in the atmosphere would rapidly break this Rossby wave down into smaller Rossby waves via the mechanism of triad resonance. However, it is impossible to predict the profile of this breakdown of the original Rossby wave because of its high dependence on the nature of the turbulence in the atmosphere, which cannot be predicted due to chaos. Such breakdown is similar to the Butterfly Effect; integration of two similar sets of initial conditions (the single Rossby wave) over periods of a day or two might yield a similar set of conditions, but completely different sets of conditions for integration over a period of a week.

Lynch wrote MATLAB code that can be used to solve the Barotropic Potential Vorticity equation that Rossby triads must obey (Equation 4.30) and integrate over a given timeframe (in units of days) to demonstrate how the energy and enstrophy, and the streamfunction of such a wave would change over time given a particular set of initial conditions (which are the three constituent Rossby waves). As the waves must be in a state of resonance for this simulation, the conditions in Equations 4.27-4.29 should be met, as should conditions for the amplitudes of the waves, discussed in Lynch's paper. His code can be use to produce three separate Rossby Waves, and superimpose them to get an initial field, a linear combination of the three constituent waves. This initial field is integrated over time to obtain a final field, and the energy and enstrophy of the triad can be followed during the course of the integration. This integration is done in the absense of turbulence - there is no stochastic component of the integration.

One can then ask a further question: How does the model behave in the presence of turbulence? This is quite a natural question to ask as due to chaotic nature of the atmosphere, a Rossby wave triad will never be free from turbulence. As the conditions for the amplitude, and the wavenumbers and frequencies of the waves required for resonance are very sensitive and specific, it is obvious that such a waveform should be unstable and therefore over a sufficiently large time period, integration of the initial field will result in a dramatically different final wave field to the final wave field in the absence of turbulence. But will the noise-free final wave field for the same period even be recognisable? There must come a point when the noise in the model, or the turbulence in the atmosphere, dominates the waveform and therefore such integration would integrate the noise, and that point may come even when the noise is significantly smaller in amplitude than the initial field.

Lynch's model considers a relatively small domain - only 61 points in the

zonal direction and 21 points in the meridonal direction. To investigate the influence of noise, a gaussian random number was added to the initial field (at each grid point) to simulate some vertical turbulence. For each integration, the amplitude of the gaussian distribution was varied to find out at what point the original stream function became no longer recognisable. While this sounds very subjective and difficult to determine when it became unrecognisable, there came a point for sufficiently large integration times where an instability arose, causing a dramatic increase in the energy or enstrophy of the simulation. Frequently, the model failed to integrate further than about a day past this point, so it was quite obvious when the noise overrode the background stream function.

Lynch's model was written in a way that it could include numerous types of initial conditions, both with and without precession of the phase of the Rossby triad. Since Lynch showed that the precession of the phase does happen in the real atmosphere, the simulation was run with the precession. This corresponds to IC type 6 in the code. The precession also gave a nice periodic oscillation of the energy and enstrophy involved in the system, with a relatively small period of oscillation whereas other initial condition types had a longer period of oscillation of these quantities which made it more difficult to identify the point at which the instability arose.

Lynch's MATLAB code is accessible from a URL that can be found in the summary of his paper [9]. This simulation was performed using his code with some small additions. Aside from adding code to draw contour plots, the only significant modification was the addition of a noise term to the stream function (see Equation 4.33 for the form of the noise), including a manual setting of the seed used for the random number generator.

The noise term added to the model was in the form

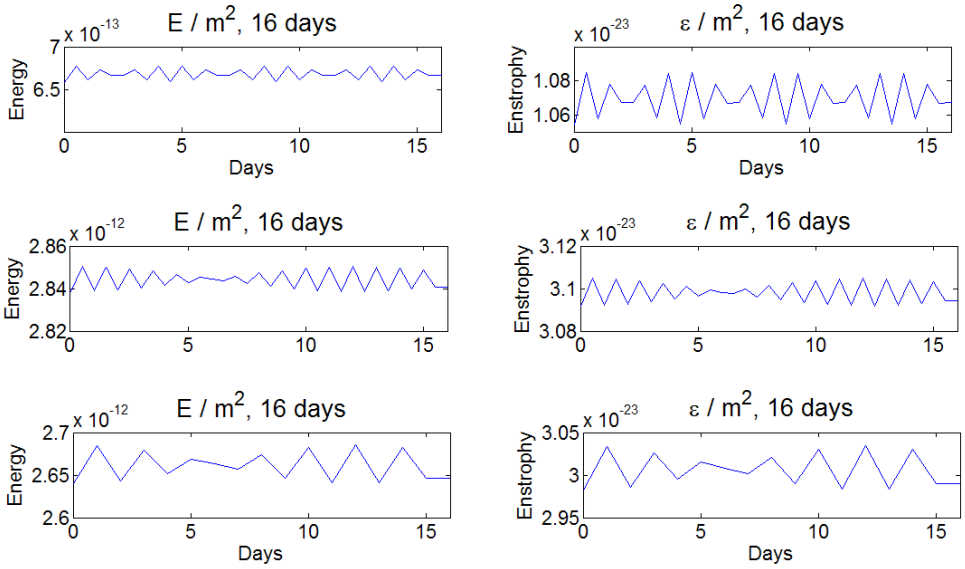

Figure 4.2: A diagram of the energy and enstrophy for several different types of initial conditions integrated over a 16-day period. Included here are IC types 7, 1 and 0 respectively of the code used to do this simulation. These IC types show a periodic oscillation that does not precess in phase. As IC type 6 does precess, it is the IC type used in the simulations. Its energy and enstrophy oscillation over a 16-day period is depicted in Fig 4.4. Not depicted is IC type 9, which leads to a spike in both energy and enstrophy after about 13 days, so is clearly too numerically unstable for a 16-day integration period. See Lynch [9] for details of the initial conditions.

$$ng\sqrt{A_1^2 + A_2^2 + A_3^2} \tag{4.33}$$

where $n = 0.1, 0.2$ or 0.3 is the noise coefficient, g is a gaussian random variable, and A_1, A_2, A_3 are the amplitudes of the three constituent waves, the solution of the Rossby triad integrated was $\psi + ng\sqrt{A_1^2 + A_2^2 + A_3^2}$. Larger noise coefficients resulted in the instabilities arising too soon for the model to be particularly useful. Smaller noise coefficients did not result in a significant deviation from the final field from the noise-free version of the final field over the time period of interest.

The integration was performed over a period of 16 days or until the instability dominated the waveform, whichever occurred sooner. Ideally an integration of a period longer than 16 days would have been used, but there was a significant change in the behaviour of the energy and enstrophy part of the model at the 16-day mark, where the baseline of these two quantities began to increase, instead of oscillating around a constant value. This change in behaviour was noticable even when allowed to run without any noise added. An integration period of longer than 16 days would have made it worthwhile to also investigate how long it took smaller noise coefficients to reach a point where they arrived at their instabilities. Only when the noise coefficient was 0.2 or 0.3 did the instability appear at a time which was not either too rapid to accurately follow how the instability developed over a long time period (i.e. the instability appeared within the first two to three days) or after the 16-day cutoff period imposed by what possibly was a limitation of the model or a result of an approximation of the numerics.

This simulation was run at a value of β corresponding to a latitude of 45° N. In order to repeat the simulation at New Zealand's latitude, only the sign of β need be changed. The zonal wavenumbers of the three waves were in the ratio of $k_1 : k_2 : k_3 = -1 : -3 : 4$, as was the case for Lynch's simulation, and meridonial wavenumbers in the ratio $l_1 : l_2 : l_3 = -1 : 1 : 0$. The third wave in the triad travelled purely in the zonal direction. It is clear that these relationships both meet the required conditions for resonance as given in Equations 4.27 and 4.28. The periods of the three individual waves were 49 days, 28 days and 18 days, meaning these are slow-moving waves with very long periods and therefore very long wavelengths. One interesting thing to note is that the integration period is shorter than the period of either of the three waves. The radius of the Earth as used in the simulation is $\frac{2}{\pi} \times 10^7$ m, which is within 0.2 per cent of the accepted value. The domain over which

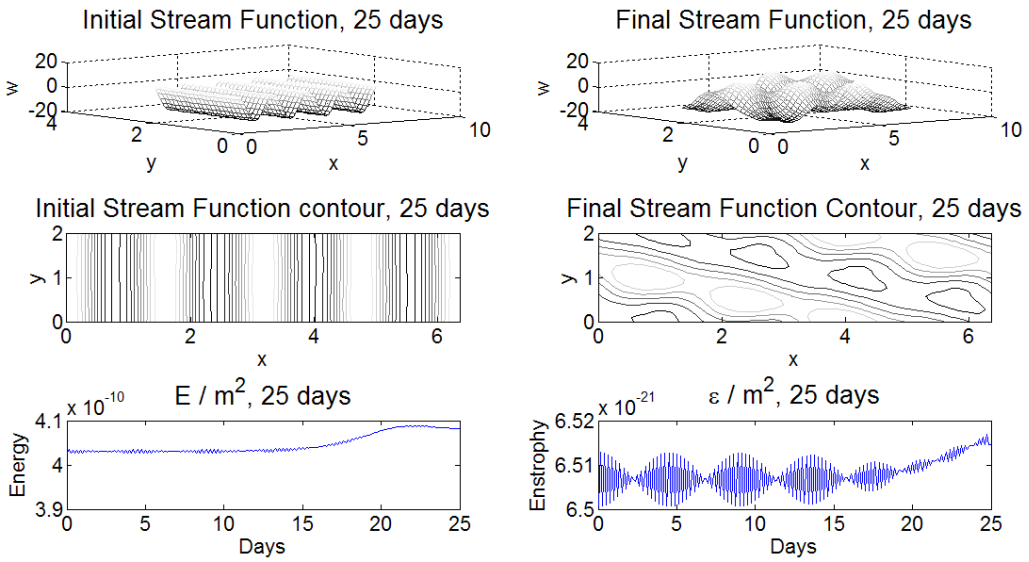

Figure 4.3: The result of performing the integration in the absence of noise for a 25-day period. The stream function integrates successfully, but there is a sudden increase in both energy and enstrophy just after the 15-day point. As the total energy in a Rossby triad must be conserved, the simulation must only be numerically valid for the first 16 days of integration, during which, the energy and enstrophy both oscillate around a constant value.

the integration was performed was a rectangular region on the surface of the earth, equal to the radius of the earth in the zonal direction and one third of the radius of the earth in the meridonial direction. There were 61 data points in the zonal direction and 21 in the meridonial direction, so each data point represented a square with a side length of a sixtieth of the radius of the Earth.

As noise was added in the form of random numbers, it was necessary to ensure the same set of random numbers was used every time the simulation was run. This was done by ensuring the same starting seed (the random number used on the first (x,y) coordinate in the integration) was used every time it was run. This is important because a different set of random numbers would result in a different appearance of the stream function as it was integrated, especially since the random numbers were included in the initial conditions of the wave, so they would have a large effect on the integration results for each

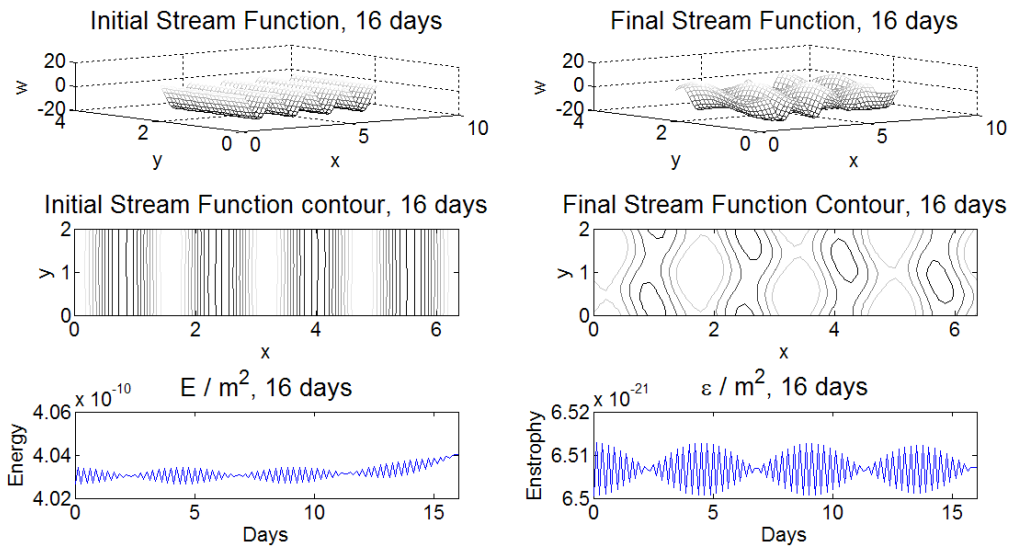

Figure 4.4: Integration of the stream function over 16 days. While the energy is starting to increase at the end of the 16-day period, the enstrophy is not yet affected. The increase in energy has not yet been dramatic, so this is an ideal time to end the integration.

point in space. It is also possible (but unlikely given there are 1281 datapoints in the simulation and therefore 1281 random numbers used, so statistically the average of the random numbers would be very close to zero regardless of the selection of random numbers) that a different set of random numbers would result in a significant change in the time when the instability is reached. This would make it more difficult to tell how the noise coefficient affects the time at which the instability arose, and therefore how sensitive Rossby resonant triads are to noise.

At the beginning of the simulation, the stream function is purely sinusoidal - it looks exactly like a wave should do. Even with the noise added, the sinusoidal structure is easily recognisable. Integrating the stream function over 16 days in the absense of noise results in a slightly distorted stream function (Figure 4.4). It is much easier to gauge how wavelike the stream function is from the contour plots. For a purely wavelike stream function, the contour plot consists of a series of straight lines, as can be seen in the Initial Stream

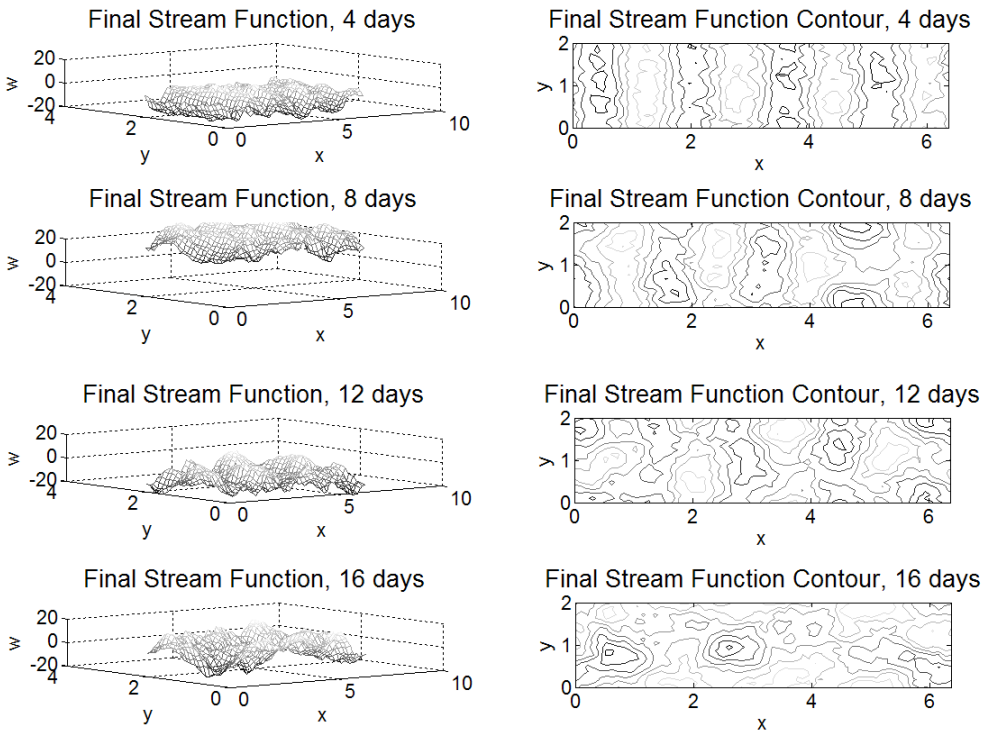

Figure 4.5: The stream-function as a three dimensional surface plot (left) and a contour plot (right) for a noise coefficient of $n = 0.1$ after 4, 8, 12 and 16 days.

Function contour plot. The energy and enstrophy both oscillate with a period of about slightly under six hours (a quarter of a day), within an envelope that is also wavelike with a period of around four days. This oscillation is centred around an energy of approximately 5×10^{-10} J m^{-2} and an enstrophy of approximately 1×10^{-19} m s^{-2}. While these are quite small values, these are waves with a small amplitude and therefore have a small energy associated with them, and are extremely slow moving waves, and therefore there is a very low amount of energy assosciated with the waves. We are more interested in the shape of the energy and enstrophy plots than the numerical values obtained.

When noise was added to the stream function, all energy and enstrophy plots assosciated with a particular noise coefficient n appear in a single figure. The corresponding stream functions appear in a separate, single figure to make

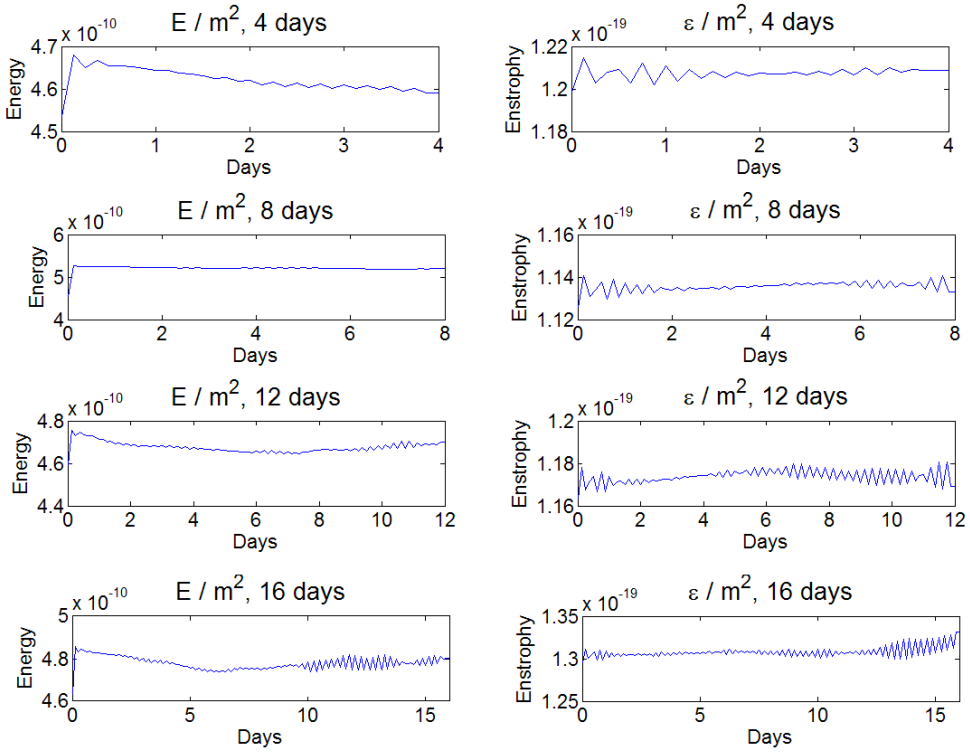

Figure 4.6: The evolution of the energy (left) and enstrophy (right) for a noise coefficient of $n = 0.1$ after 4, 8, 12 and 16 days.

it easier to see how these quantities evolved as the integration proceeded (e.g. Figures 4.5 to 4.10).

Even on adding noise, it can be seen from Figures 4.6, 4.8 and 4.10 that the energy and enstrophy both retained their oscillations with a period of six hours, but the wavelike envelope with a period of 4 days was lost. The noise clearly only has an effect on the envelope of the energy and enstrophy, and the six-hour oscillation is a fundamental property of the Rossby triad - perhaps related to the transfer of energy between its three constituent waves.

With a noise coefficient of $n = 0.1$, after 4 days the stream function can still be easily recognised as a wave (Figure 4.5). It is towards the end of the integration that it begins to lose its sinusoidal structure as the noise that was added to the original stream function before the integration began begins to

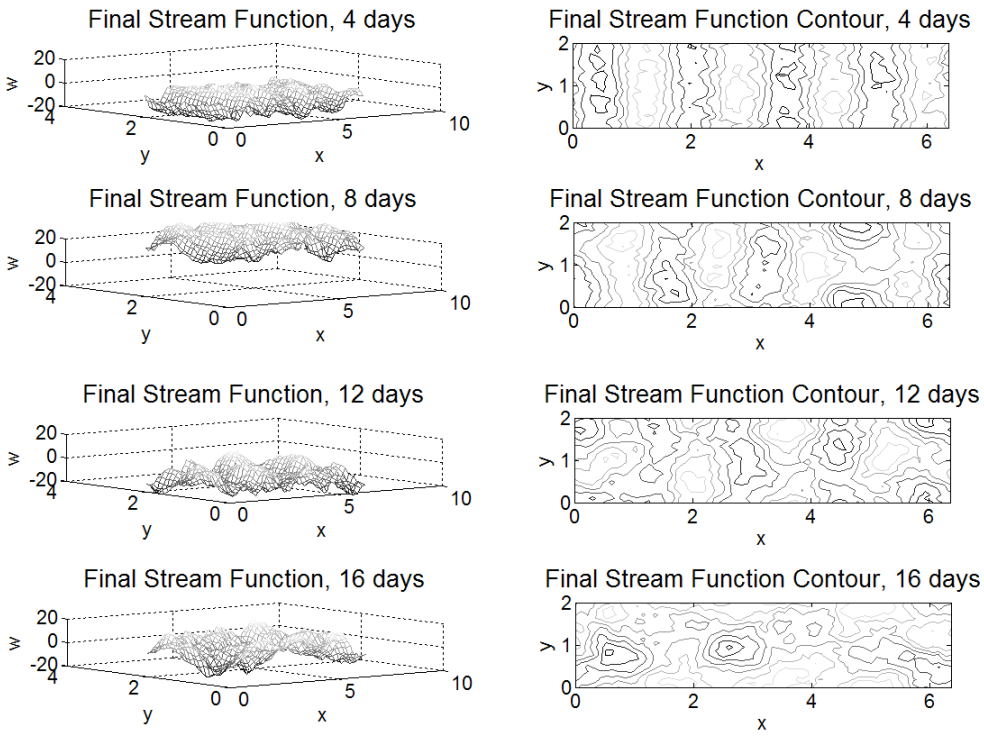

Figure 4.7: The stream function as a three dimensional surface plot (left) and a contour plot (right) for a noise coefficient of $n = 0.2$ after 4, 8 and 12 days. The instability arises just after 10 days, as is evident from the corresponding energy and enstrophy plots.

dominate the stream function, but it is not so dominant that the numerical instability is reached during the period of integration. At the end of the 16 days the stream function has peaks and troughs randomly distributed around the domain of the integration.

The energy plots corresponding to $n = 0.1$ (Figure 4.6) are very different to those without noise. After spiking several hours into the integration, the energy per square metre slowly decreases in value by less than one per cent over the first eight days and then increases slightly after this point. It does not oscillate around a particular value like the no-noise case did. The amplitude of the six-hourly oscillations increased as the integration went on, a possible indication of the noise becoming more dominant as time passes. The enstrophy on the other hand, was closer to being constant, with only an apparent

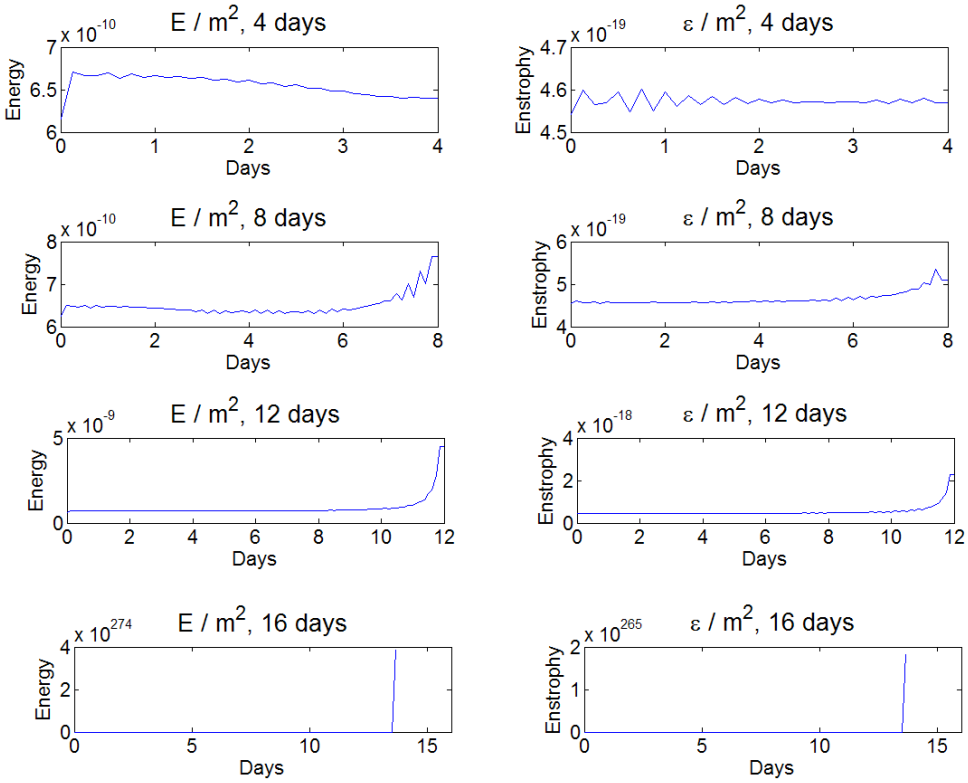

Figure 4.8: The evolution of the energy (left) and enstrophy (right) for a noise coefficient of $n = 0.2$ after 4, 8 and 12 days. It is obvious that the instability occurs around the tenth day of the integration.

very small overall increase during the course of the integration. This increase is just a result of the selection of random numbers used in this run of the simulation - running the same simulation with different seeds did not yield the same increase.

A noise coefficient of $n = 0.2$ was the lowest value tested that arrived at the instability during the sixteen day integration period, and this occurred at around the twelfth day.. The point at which the instability was reached is obvious from the (unphysical) increase in both energy and enstrophy at this time, which can be seen in the lower two plots of Figure 4.8. Because of the unphysical nature of this energy increase, it is almost certain that this instability is a numerical one, and integration after twelve days is no longer valid. Prior to this point, the sinusoidal form of the stream function is barely recognisable

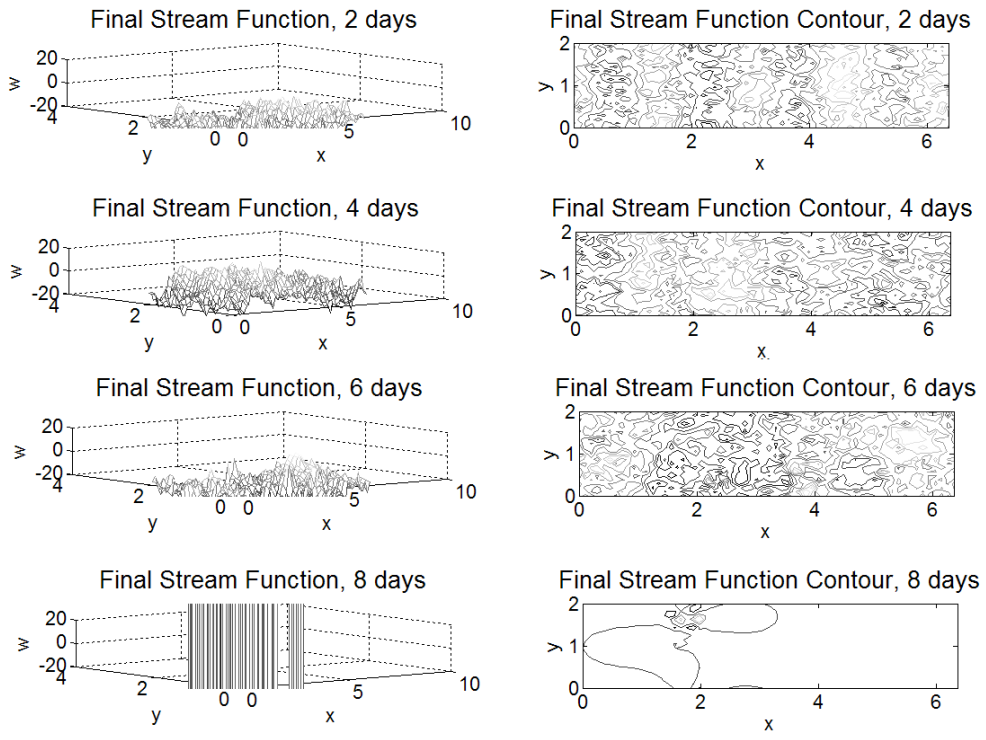

Figure 4.9: The stream function as a three dimensional surface plot (left) and a contour plot (right) for a noise coefficient of $n = 0.3$ after 2, 4, 6, and 8 days. The instability is reached on the eighth day of integration.

after four days and the noise dominates the stream function after eight days.

During the first four days of integration, the energy and enstrophy both behaved as they did with a noise coefficient of $n = 0.1$, although the values are a little higher. Between the sixth and eighth day of integration, both values start to increase, however the increase in energy is much more dramatic. After eight days of integration, this increase has only reached about twenty per cent of the original value in energy, but by the twelfth day it has increased by a factor of approximately 10^{19}.

For a noise coefficient of $n = 0.3$, the instability was reached on the eighth day. Because of the shorter period between commencement of integration and the instability, as well as the more rapid evolution in stream function, the stream function is plotted every two days instead of every four, as was the

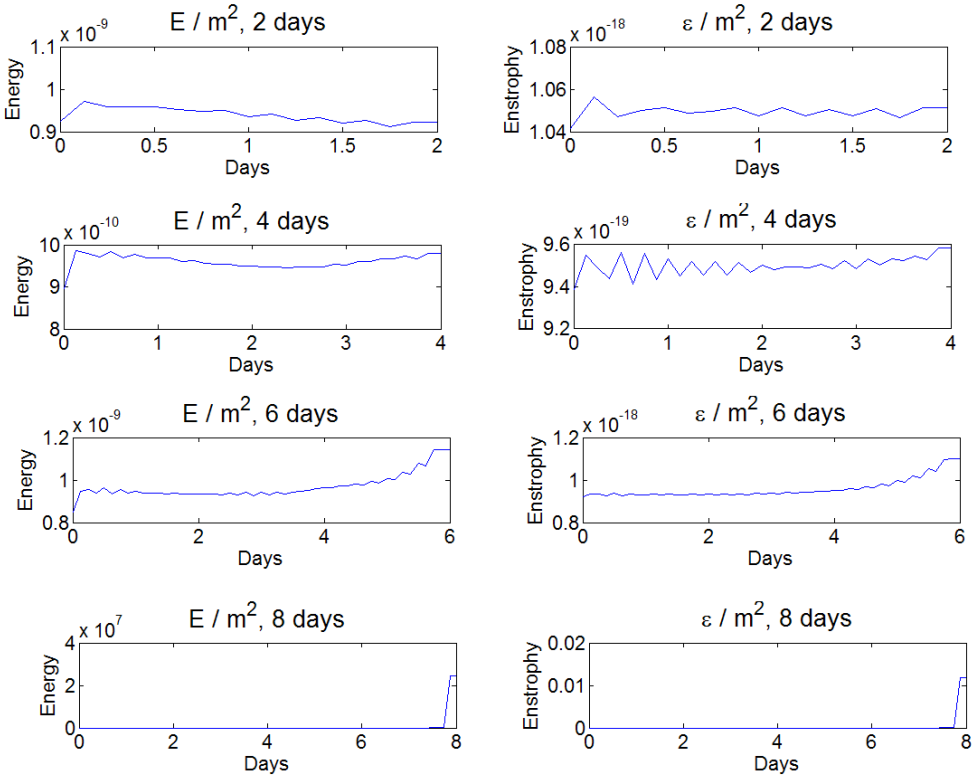

Figure 4.10: The evolution of energy (left) and enstrophy (right) for a noise coefficient of $n = 0.3$ after 2, 4, 6, and 8 days. It is obvious that the instability is reached on the eighth day of integration.

case in the previous runs. After two days the sinusoidal form of the stream function is barely recognisable. After six days, the noise dominates the stream function and it loses its sinusoidal shape. After 8 days, by which time the instability has been reached, there are only one or two peaks but they are huge - using the same scale that the earlier plots were drawn on, the peaks appear as a series of vertical lines. Because the energy and enstrophy associated with this stream function increases in an unphysical manner, this particular stream-function must also be unphysical - again, the instability is probably numeric.

We will now have a closer look at the processes that take place just before the instability is reached. In Figures 4.11 and 4.12, the stream function and the energy and enstrophy are plotted every six hours between 6.5 days into the integration and 7.75 days into the integration, with a noise coefficient of 0.3.

Interestingly we see that the values around which the stream function is centred decreases in value between the 6.5 day plot and the 6.75 day plot and then returns to normal before the end of the seventh day. At around the same time, the number of peaks and troughs in the stream function begins to decrease as is evident from the less cluttered contour plots in Figure 4.11 from the end of the seventh day and into the eighth day. The actual instability manifests itself rapidly around 7.5 days, so if one were to only look at the results of the first seven days of integration they would not find it obvious that the arrival at the instability is imminent. The sudden rapid onset of the instability is also apparent from Figure 4.12, where there is an extremely sharp increase in both energy and enstrophy after 7.5 days.

The energy and the enstrophy obtained in the model is not an overall value for the entire domain of the wave, it is instead a value obtained per square metre - in order to calculate the overall energy and enstrophy of the waves it is necessary to multiply by the area of the domain of the integration. Very small values of both quantities were obtained, but this is to be expected since waves of very small amplitudes were used for the simulation. Also, one wave in the triad had a much larger amplitude than the remaining two. While Rossby waves of larger amplitude do indeed exist in the atmosphere, the purpose of this simulation was to examine the total energy and enstrophy of the triad. Larger amplitude waves tend to dissipate energy faster whereas lower amplitude waves tend to retain their energy, making them better for the purposes of the simulation.

This model, however has several limitations that need to be addressed. The model assumes the noise has an effect in the vertical direction only, as the noise term is only added to the initial stream function waveform. Turbulence is going to have effects in the horizontal direction too, which means a noise term should also be added to to the arguments of the cosine terms. This

would likely result in the models reaching instabilities sooner. The horizontal effects of turbulence could well have more dramatic effects over the course of the integration than the vertical ones do.

It also only accounts for noise that is there initially - at the beginning of the integration. It is possible that some turbulence will arise during the time period of integration where at the beginning of the integration there is not even the smallest hint of turbulence at a particular location in the domain of integration. In order to account for this in the model, perhaps it may have been beneficial to not only add noise to the model at the beginning of the integration but also add some noise by adding random numbers to the model during the course of the integration, approximating a random forcing such as wind.

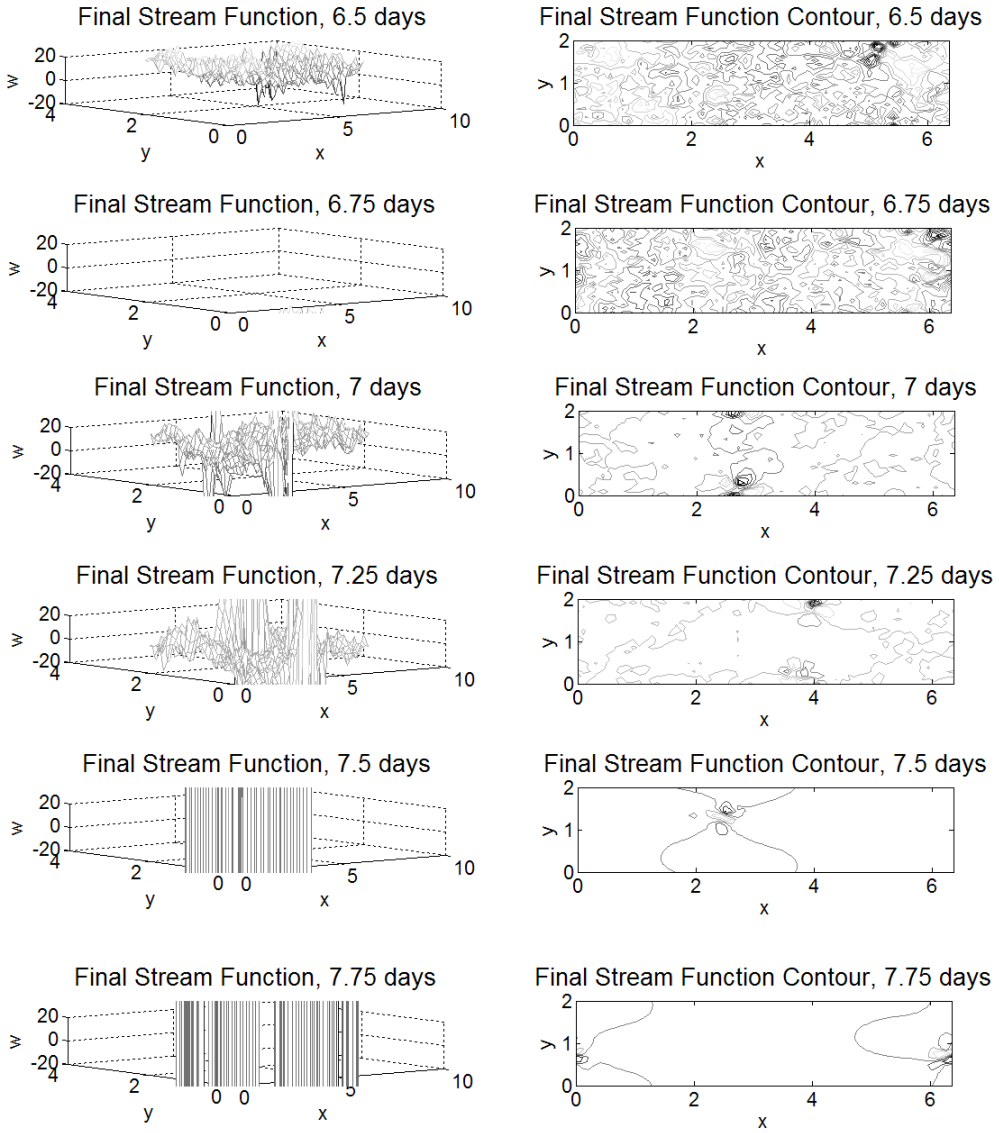

Figure 4.11: The evolution of the stream function as a three dimensional surface plot (left) and a contour plot (right) approaching the point the instability is reached. In this case the noise coefficient is $n = 0.3$ and the stream function is viewed at 6-hourly intervals starting at 6.5 days into the integration and ending 7.75 days into the integration, however the appearance of the stream function for a noise coefficient of $n = 0.2$ is similar even though the stream function is reached later in that case.

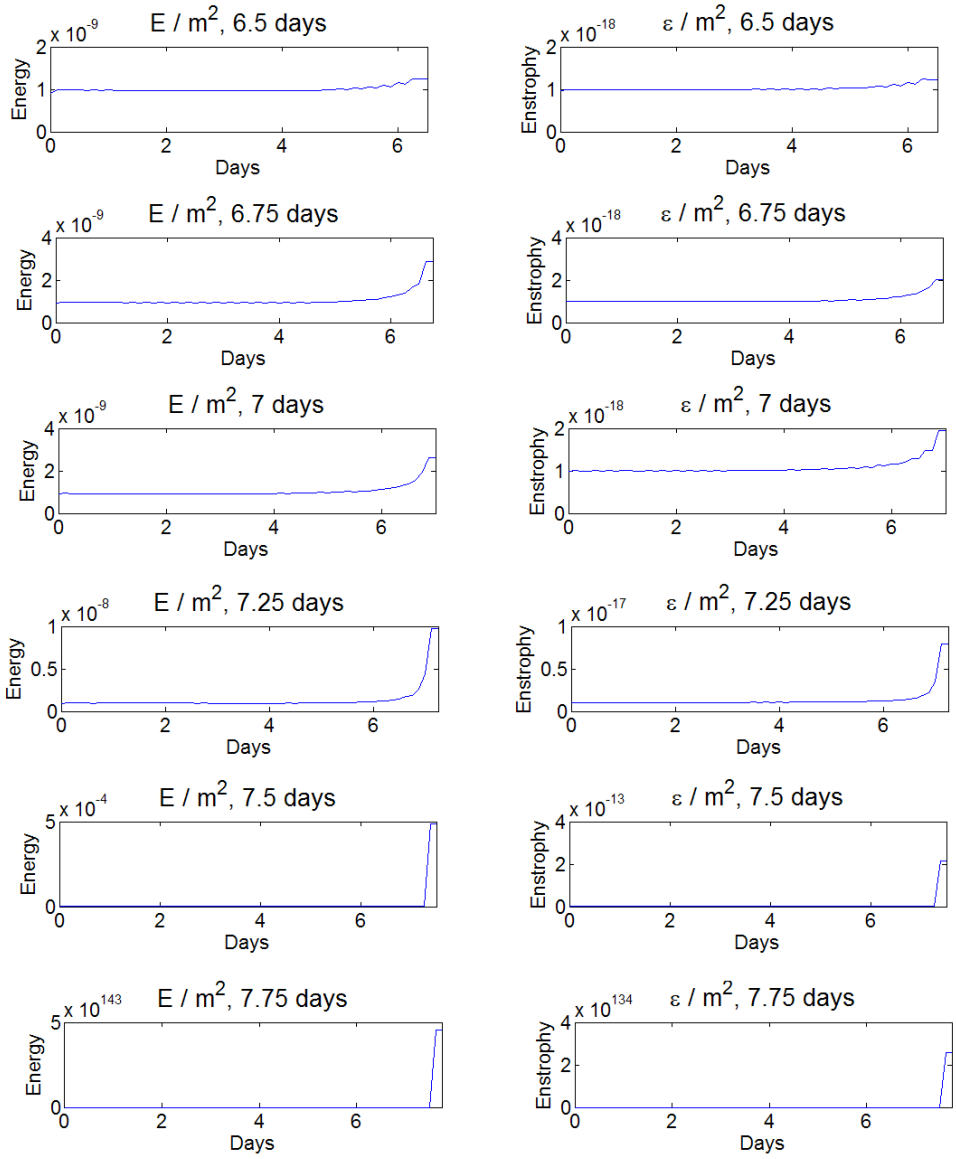

Figure 4.12: The evolution of the energy and enstrophy approaching the point the instability is reached. As with the plot involving the stream functions at the same point in the integration periods, the noise coefficient is $n = 0.3$ and the graph took on a similar shape to those of noise coefficient 0.2 during the point its instability was reached.

Chapter 5

Kelvin Waves

Kelvin waves were discovered by Sir William Thomson (also known as Lord Kelvin) in 1879 [14]. They are in general nondispersive waves, so their group speed is equal to their phase speed. Kelvin waves exist in both the atmosphere and the ocean. Here we will firstly consider their motion in the ocean to see how they behave. While atmospheric Kelvin waves will not be deflected by the coastline like their oceanic counterparts, they can be deflected by mountain ranges that are oriented close to a north-south direction near the equator. An example of such a mountain range is the Andes, in South America.

It is known that Kelvin waves are nondispersive waves, which means that all parts of a Kelvin wave propogate with the same velocity, and therefore a Kelvin wave retains its shape as it propagates.

Kelvin Waves are a kind of gravity wave. They would not be able to exist without the gravitational attraction of the Earth. They also need geographical boundaries, such as coastlines, mountain ranges to exist. They also need significant Coriolis acceleration which implies they do not form at the equator. In fact the equator provides yet another boundary. Kelvin Waves never pass through the equator from one hemisphere to the other but they travel eastward along the equator, meaning they do not obey the no-slip boundary condition

there. The equator acts as a waveguide for such waves.

While they do not form at the equator, they have their largest amplitude ther, decaying exponentially as the latitude increases on either side. Kelvin Waves always travel in a cyclonic manner. That is, they travel towards the equator along western boundaries and towards the poles on eastern boundaries.

There are two main kinds of Kelvin Wave, equatorially trapped Kelvin Waves (that as we mentioned before, travel in a purely eastward direction) and Coastally trapped Kelvin Waves. Here we will consider the motion of a Kelvin wave as it encounters a purely meridonal (north-south) coastal boundary.

Oceanic Kelvin waves are not prevalent in or around New Zealand, due to the fact that NZ lies far from the equator or any north-south boundaries that extend as far as the equator.

For both these cases, let us assume the atmosphere moved at constant speed. Let us take u to be the speed in the west-east direction and v to be the speed in the north-south direction.

Here we will only discuss Equatorially trapped Kelvin waves. These waves cause and have an effect on weather-related phenomena such as El Nino and La Nina, which we shall see in the next chapter. In order to build up to such a point where it is possible to discuss the causes of these phenomena, it is necessary to look at equatorially trapped Kelvin Waves in both the ocean and the atmosphere.

Since the equator is a boundary, and Kelvin Waves cannot penetrate it, at the equator there will be no north-south component of motion and therefore

$v = 0$. We also need to use the Beta-plane approximation, and since $f_0 = 0$ at the equator this approximation reduces to $f = \beta y$. We will consider Kelvin waves in the two horizontal dimensions, assuming that a Kelvin wave's motion is purely horizontal. While a kind of Kelvin wave that propogates vertically does exist, we are going to ignore such waves for the purposes of this discussion.

5.1 Oceanic Equatorial Kelvin Waves

Kelvin waves are gravity waves. They are subject to several equations of motion .If g is the acceleration due to gravity experienced by the wave, and h_0 is the characteristic height of the wave, then the motion of the wave is subject to the three equations (see Vallis, page 17 [15])

$$\frac{\partial u}{\partial t} + g\frac{\partial h}{\partial x} = 0 \tag{5.1}$$

$$\beta y u + g\frac{\partial h}{\partial y} = 0 \tag{5.2}$$

$$\frac{\partial h}{\partial t} + h_0\frac{\partial u}{\partial x} = 0 \tag{5.3}$$

We can anticipate the solution will be of the form

$$h = Ae^{i(kx-\omega t)} \tag{5.4}$$

which is the usual form of a wave travelling purely parallel to the equator. The amplitude depends on the latitude, i.e. $A = A(y)$.

Taking the time derivative of Equation 5.3 gives

$$\frac{\partial^2 h}{\partial t^2} + h_0\frac{\partial^2 u}{\partial x \partial t} = 0 \tag{5.5}$$

and taking the spatial (x) derivative of Equation 5.1 gives

$$\frac{\partial^2 u}{\partial x \partial t} + g\frac{\partial^2 h}{\partial x^2} \tag{5.6}$$

Multiplying Equation 5.6 through by h_0 and subtracting from Equation 5.5 yields the wave equation

$$\frac{\partial^2 h}{\partial t^2} - gh_0\frac{\partial^2 h}{\partial x^2} = 0 \tag{5.7}$$

and comparing with the well-known form of the wave equation tells us that $c^2 = gh_0$, or $c = \pm\sqrt{gh_0}$ is the phase speed. This is equivalent in form to the shallow water wave phase speed. It has been found that the typical phase speed of Kelvin waves in the the uppermost layer of the ocean near the equator is in the order of 2-3 ms^{-1}.

But we now need to calculate the form of the dependence of the amplitude on the latitude, in other words ascertain the function $A(y)$.

Noting that the y coordinate is constant, taking the time derivative of Equation 5.2 and simultaneously dividing through by g results in

$$\frac{\beta y}{g}\frac{\partial u}{\partial t} + \frac{\partial^2 h}{\partial y \partial t} = 0 \tag{5.8}$$

Also, multiplying Equation 5.1 through by $\frac{\beta y}{g}$ results in

$$\frac{\beta y}{g}\frac{\partial u}{\partial t} + \beta y\frac{\partial h}{\partial x} = 0 \tag{5.9}$$

Subtracting equation 5.9 from 5.8 results in

$$\frac{\partial^2 h}{\partial y \partial t} = \beta y \frac{\partial h}{\partial x} \tag{5.10}$$

We already know the form of h from the derivation of the phase speed; substituting this form into Equation 5.10 and simplifying results in

$$-\omega A' = k\beta y A \tag{5.11}$$

where $A' \equiv \frac{dA}{dy}$. This is a separable differential equation; solving via separation of variables yields

$$A = A_0 e^{\frac{-k\beta y^2}{2\omega}} \tag{5.12}$$

But we can substitute in the phase speed: $\frac{\omega}{k} = \sqrt{gh_0}$, resulting in

$$A = A_0 e^{\frac{-\beta y^2}{2\sqrt{gh_0}}} \tag{5.13}$$

Defining L_{eqd}, the equatorial deformation radius, by

$$L_{eqd}^2 = \frac{2\sqrt{gh_0}}{\beta} \tag{5.14}$$

this can be written

$$A = A_0 e^{-\frac{y^2}{L_{eqd}^2}} \tag{5.15}$$

and therefore an oceanic equatorial Kelvin wave has the solution

$$h = A_0 e^{-\frac{y^2}{L_{eqd}^2}} e^{i(kx-\omega t)} \tag{5.16}$$

This is how oceanic Kelvin Waves behave in the middle of the ocean, nowhere near any land masses. A different kind of behaviour results when the waves meet a land mass. In such a situation, the coastline acts as a waveguide, deflecting the waves to the north or the south (depending on which hemisphere the wave is in - it is always deflected away from the equator). As this occurs, they cease to become equatorially trapped Kelvin waves, and become coastally trapped Kelvin waves.

5.2 Atmospheric Equatorial Kelvin Waves

We begin our analysis of atmospheric Kelvin waves by looking at Lindzen's 1967 paper "Planetary Waves on Beta Planes" [7] in conjunction with Holton and Lindzen's 1968 paper "A Note on 'Kelvin' Waves in the Atmosphere" [6].

Treating the atmosphere to be fluid of uniform density ρ_0, with u and v being the two horizontal velocity components, then take

$$u' = \sqrt{\rho_0}u \tag{5.17}$$

$$v' = \sqrt{\rho_0}v \tag{5.18}$$

Unlike with the Rossby dispersion relationship derivation we are assuming here that we are dealing with an air parcel located wholly at a particular latitude, which has constant density, which justifies the constant density assumption whereas we had a variable density in the Rossby waves case. Equations 10 and 11 of the 1967 paper [7] state, using the beta plane approximation, and defining δp to be a pressure oscillation

$$i\omega u' - (f_0 + \beta y)v' = -ik\delta p \tag{5.19}$$

$$i\omega v' + (f_0 + \beta y)u' = -\frac{\partial}{\partial y}\delta p \tag{5.20}$$

In the absense of meridonial flow (i.e. $v' = 0$), these equations reduce to

$$\omega u' = -k\delta p \tag{5.21}$$

$$(f_0 + \beta y)u' = -\frac{\partial}{\partial y}\delta p \tag{5.22}$$

At the equator, $f_0 = 0$. Solving the former equation for δp and substituting into the latter yields

$$\beta y u' = \frac{\omega}{k}\frac{\partial u'}{\partial y} \tag{5.23}$$

which is the condition required for a nontrivial solution. This differential equation is readily solved via separation of variables:

$$\frac{du'}{u'} = \frac{k\beta}{\omega} y dy \tag{5.24}$$

and integration results in

$$u' = F(z)\exp(\frac{k\beta y^2}{2\omega}) \tag{5.25}$$

on realising that the amplitude of such waves is not necessarily uniform, but can instead depend on z, the vertical coordinate. We can then write this as

$$u = G(z)\exp(\frac{k\beta y^2}{2\omega}) \tag{5.26}$$

where

$$G(z) = \frac{F(z)}{\sqrt{\rho_0}} \tag{5.27}$$

Note also that ρ_0 does depend on the altitude the wave is travelling at. $F(z)$ is an unknown function of the altitude so we can conclude that the height of the Kelvin wave of interest does depend on the height. At the equator, $y = 0$ and the amplitude reduces to

$$u = G(z) \tag{5.28}$$

so the function $G(z)$ describes the profile of the velocity of the wave at the equator. Intuitively, this is expected to be a monotonically decreasing function since, at low values of z, as the atmosphere is more dense, the air particles are going to be close together, which is conducive to a medium-requiring wave travelling through them efficiently and quickly, however the particles are sparser at higher latitudes, resulting in a less efficient transfer from one particle to the next. We also expect the wave to dissipate faster at higher latitudes as a result of this inefficient transfer of energy.

This is a kind of Kelvin Wave known as an *internal* Kelvin wave. Such Kelvin waves do move in the middle of a medium (i.e. not at any surface) but their motion depends on the density of the fluid where they propagate, which in turn means their motion varies with depth within the fluid. The other kind

of Kelvin wave is one that propagates along the surface of a medium. The most obvious example of a surface Kelvin wave is one that propagates along the atmosphere-ocean interface.

Chapter 6

The Walker Cell and El Niño Southern Oscillation

The El Niño Southern Oscillation, also known as ENSO, is a weather phenomenon that is governed by a cycle which repeats approximately once every three to seven years. It consists of a colder part of the cycle and a warmer part of the cycle.

Typically, the air pressure at the equator is slightly lower than the air pressure either side of the equator, due to the Coriolis force near the equator deflecting some of the air to the north and south of the equator. As the atmosphere aims to balance any pressure gradients this results in a wind blowing in a direction towards the equator, but typically has a nonzero component of velocity parallel to the equator. Under normal circumstances, this parallel component is in the westward direction. This results in a southeasterly wind in the southern hemisphere, and a northeasterly wind in the northern hemisphere. These winds are known as the "trade winds". These trade winds occur during "normal" conditions (which are neutral conditions, at a time when neither El Niño or La Niña is present). La Niña is caused by a strengthening of the trade winds, whereas El Niño occurs when these trade winds cease to blow, or even reverse in direction.

The information to follow about the mechanism of ENSO follows a video series on El Niño created by Sakagami [13]. Wind friction from these easterly trade winds drag some of the water on the surface of the ocean to the western Pacific, meaning that the sea surface becomes higher in the western pacific than it does in the eastern Pacific. Since gravity acts to equalise this height gradient, it tries to push the water east, while the wind is trying to push the water west. However the wind friction is pushing the water west, so there exists an (unstable) equilibrium of forces between gravity and the wind.

But, while the wind is pushing west, the atmosphere is a turbulent system, so there are times when a localised region of airflow is travelling eastward. This is especially so when one considers that the zonal component of the trade winds blows against the Kelvin waves, and these waves act to further disrupt the unstable equilibrium of forces. When this happens, the gravity-wind equilibrium becomes upset, and a wave of water is sent travelling eastward. These waves are known as oceanic Kelvin waves. Usually, the force equilibrium can recover before a significant volume of water migrates east, and no major consequences occur. However this recovery does not always occur, and when it fails to recover, it starts a chain of events that marks the beginning of an El Niño phase.

The 20° thermocline is a layer of water in the equatorial Pacific ocean lying below the surface of the ocean where the temperature is 20° C. Usually, this is near the surface in the eastern Pacific, whereas it is quite deep in the west.The 20° C thermocline usually tilts in the opposite direction to the surface. But as water moves east, both the surface and the 20° thermocline lose their gradients and become horizontal. This means it is at a shallower than normal depth at the western Pacific, but deeper than usual at the east. This results in upwelling in the east, which makes the air pressure of the eastern pacific drop and the pressure gradient between the two sides of the Pacific diminishes. As

a result, the trade winds die down, meaning there is no significant air flow over the Pacific Ocean on a large scale. Sometimes, the air pressure at the eastern Pacific drops below that of the western Pacific, meaning the prevailing winds reverse in direction.

The state of the Pacific Ocean being level during El Niño is stable but abnormal. Eventually, if the El Niño phase continues, the water can no longer travel east, so it is deflected to the north, or south (i.e. away from the equator), causing this water to cool, and so does the air above it, so it increases in pressure until it reaches a pressure greater than the pressure at the western Pacific. At this point, an easterly wind develops and strengthens. Once the wind becomes sufficiently strong, the wind forces a large volume of water back to the western Pacific, with the result that the unstable but usual sea level-wind asymmetry is restored. But the recovery process usually overshoots, causing more water than necessary to migrate west and the easterly wind to initially become much stronger than necessary, initiating a La Niña phase. This is why an El Niño year is usually immediately followed by a La Niña year.

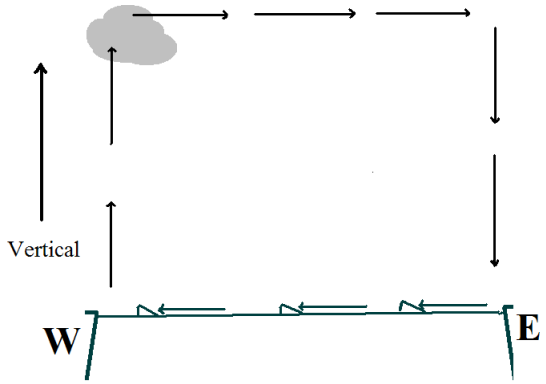

Figure 6.1: A schematic of the Walker Cell. The left hand side of the figure is the western Pacific; the right hand side is the eastern Pacific. At sea level, the wind blows from east to west, dragging some of the water from east to west. Once it reaches the western side of the Pacific, it rises due to the fact that it is warmer, moist air. As it rises, its saturation point decreases, meaning some of the moisture is lost. It then returns to the eastern Pacific, where it descends to complete the circuit.

Darwin is slightly closer to the equator than Tahiti is, and therefore the air pressure at Tahiti is normally slightly larger than the air pressure in Darwin, which results in an easterly wind blowing across the tropical Pacific, from Tahiti to Darwin. As these winds cross the Pacific Ocean, a large source of warm water, which means the air becomes saturated with warm water vapour. Once these winds reach Darwin, this causes the air to rise, and as it does so it loses some of its capacity to carry water vapour. This results in the formation of cumulonimbus clouds above Darwin, with extensive precipitation in the area. Once the air completes its ascent, it moves back toward Tahiti, until it descends and the process repeats.

This circuit the air traverses between Tahiti and Darwin is known as the Walker cell, named after Sir Gilbert Walker, who accidentally pieced together ENSO while researching the mechanism of monsoons on the Asian subcontinent in the early 20th century.

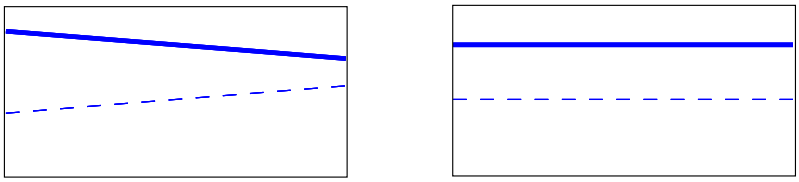

Figure 6.2: A diagram showing the usual slope of the Pacific Ocean . In non El Niño conditions (left), the ocean surface (represented by the solid line) is higher in the western Pacific whereas the 20° C thermocline (dotted line) is lower. In El Niño conditions (right), both the surface and the 20° C thermocline become level as a result of a large volume of water to the east.

ENSO is important to meteorologists because it can have a marked effect on industry. It is therefore important that the timing of the ENSO is predicted as accurately as possible. We will soon see that predicting ENSO accurately is very difficult.

While weather conditions in New Zealand and Australia are not influenced

by ENSO as much as countries like Peru (where flooding is regular in El Niño years), it does have a significant effect. However, the El Niño phase of the ENSO scale has a stronger effect on New Zealand, than the opposite extreme, La Niña.

El Niño subjects New Zealand to stronger westerly winds in the summern months, which results in more rain in western New Zealand, while eastern New Zealand experiences drier conditions. Winter conditions in El niño years tend to be colder than other years, because the wind comes from a more southerly direction, so New Zealand and the surrounding ocean is subjected to the cold air from Antarctica. As is to be expected, autumn and spring conditions, which intuitively lie between the extremes of winter and summer conditions, consist of southwesterly winds.

The other extreme of the ENSO cycle is the La Niña phase. Typically New Zealand experiences noth-easterly winds during the La Niña phase, resulting in wetter conditions for the north-eastern part of the country, while the west coast of the South Island experiences drier than usual conditions. Some of the central South Island, like central Otago, and South Canterbury are subject to drier than usual conditions during both extremes of the ENSO cycle, especially during the summer months.

But ENSO is not the main culprit for the year-to-year climate variation New Zealand experiences. In fact, it only accounts for about a quarter of the annual variation that exists in New Zealand rainfall and temperatures. While the aforementioned droughts often occur in eastern NZ during El Niño summers, they do not necessarily occur every El Niño phase of the cycle, and these droughts can also occur outside El Niño periods. Also the areas most heavily affected by these droughts are not the same every time. There are some areas more consistently affected than others, but even these areas are not necessarily

hit to the same extent every time.

One of the most significant ENSO events in recent history took place in between April 1997 and June 1998 [16]. El Niño conditions became prevalent during the second quarter of 1997, causing major weather-related disasters around the world including drought in Papua New Guinea (resulting in a shortage of food because the crops did not have sufficient water to grow), bushfires in Australia and Indonesian tropical forests, and fires in Venezuela, French Guyana and Brazil. Conversely, there were an unusually large number of tropical cyclones in the south Pacific between October 1997 and April 1998, with significant flooding in Ecuador, Peru and Chile. While Venezuela, French Guyana and Brazil are somewhat of an anomaly, the obvious trend is drier conditions in the western Pacific, but wetter conditions in the eastern Pacific.

The Southern Oscillation Index (SOI) is a method used for indicating whether El Niño or La Niña conditions are prevalent at any given time. It is is based on taking the difference in air pressure between two points, namely Darwin and Tahiti. A highly positive value of the SOI indicates strong La Niña conditions, whereas a highly negative SOI indicates strong El Niño conditions. SOI values between -8 and +8 are said to be neutral ENSO conditions, At the time of writing, the SOI has a value of approximately +22, indicating strong as Niña conditions, and the SOI has been consistently positive for over a year (since April 2010).

There are a few variations in the method employed to calculate the SOI. One such method is known as the Troup SOI, which is used by the Australian Bureau of Meteorology. They calculate the SOI for each calendar month using the following formula:

$$SOI = 10\frac{P_T - P_D - P_{Diff,av}}{\sigma_{Diff}} \tag{6.1}$$

where P_T is the air pressure at sea level in Tahiti for the month, P_D is the air pressure at Darwin for the month, $P_{Diff,av}$ is the average difference (Tahiti minus Darwin) for the same month of the year over previous years, and σ_{diff} is the standard deviation of the pressure difference for the same month of the year over previous years.

There are several other algorithms used to measure the current state of ENSO. These include the Nino3 and Nino4 indices, as well as the Nino3.4 index. Here we will discuss the Nino3.4 index.

The Nino3.4 index is based on the average sea surface temperature of a rectangular region in the Pacific ocean, bounded by the lines of latitude 5° N and 5° S, and the lines of longitude 170° W and 120° W. The Nino3.4 index is the difference between the sea surface temperature and the average sea surface temperature for each month, measured in degrees Celsius. Currently, the average used was calculated over the 30-year period from January 1961 to December 1990. By convention, a La Niña event occurs where the 5-month running average of the Nino3.4 index is greater than +0.4, and an El Niño event occurs when the 5-month running average is less than -0.4. A running average is used to ensure that a short-term fluctuation in sea surface temperature is not interpreted as being a long-term event.

6.1 Predictability of ENSO

People have been attempting for many decades to predict when an El Niño or a La niña event would occur, in order to give the maximum possible warning

Figure 6.3: The rectangular region, in solid black, over which the average sea surface temperature is taken, for the Nino3.4 index. This region is directly to the west of Columbia. The northern edge is at a latitude of 5^o N; the southern edge at 5^o S; the western edge at a longitude of 170^oW and the eastern edge at 120^0 W.

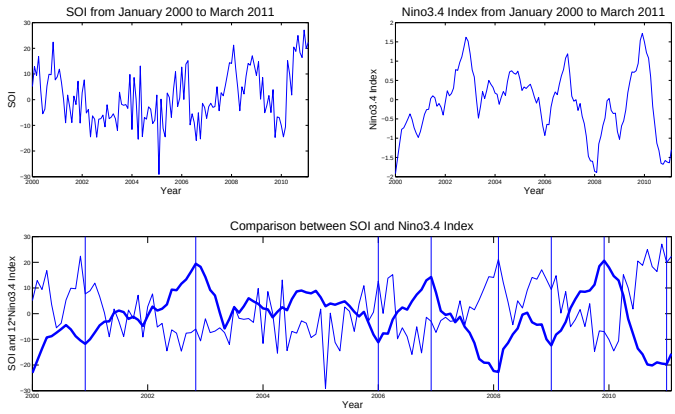

Figure 6.4: A plot showing the SOI index as a function of time, using monthly data from January 2000 to March 2011 (top left). A plot showing the Nino3.4 index over the same time period (top right). The bottom plot is a comparison of both plots overlaid. Note that El Niño occurs when the SOI is negative but the Nino3.4 index is positive. But the two plots overlaid shows that the peaks in the SOI plot coincide with the peaks in the Nino3.4 plot, demonstrating the two indices are consistent with each other, as they should be. The thicker line is the Nino3.4 index, which has had its amplitude multiplied by 12 in order to enable a comparison between the two indices. Highlighted peaks are the ones with a vertical line through them, they occur in December 2000, November 2002, January 2006, December 2006, February 2008, January 2009, December 2009 and January 2011. The graphs show that the is a significant La Niña event in early 2011. The data used for plotting this figure was obtained from the Bureau of Meteorology, Australia [2].

time that such an event will happen so the public can prepare for it so its negative effects can be less destructive. But this is, in practice, a very difficult thing to do, mostly because of how the onset of an ENSO event is brought about by turbulence in the atmosphere, and the inability of the aforementioned equilibrium of forces to recover before a large quantity of water migrates to the eastern side of the Pacific. Since 1900, there have been 26 different El Niño events [2]. The time period between two consecutive events has ranged from two years (on four occasions) to ten years (from 1941 to 1951). People are not only interested in predicting when an event will occur, but also the severity of an event - they want to know how serious the effects of an event will be, and how long it will last. But again, this is very difficult to predict.

Several different models have been proposed. One such model was proposed by Federov et al in 2003 [4], where the Southern Oscillation was compared to the oscillation of a giant pendulum across the Pacific Ocean. It was argued that the motion of the water across the Pacific from east to west is analogous to the motion of a plumbob from east to west. They believed that in the absence of turbulence the Southern Oscillation would be purely periodic, and extremely predictable, just like the motion of a pendulum. The pendulum considered in the model is one that is exposed to wind that blows in the direction of the plane of the motion of the pendulum. More specifically, only westerly winds are considered.

Not only is the model used to describe the timing of the peak of El Niño and La Niña, it is also used to describe how intense each ENSO event is. This part of the analogy is drawn from the amplitude of each swing; the larger the amplitude, the more intense an event is. It is used to explain how some gusts of wind can trigger an ENSO event and others do not. In the pendulum analogy, a gust of wind transfers energy to the pendulum when the pendulum is swinging in the same direction as the wind, which gives the swing a larger

amplitude, and the pendulum travels a larger distance to the east. However, a gust of wind that acts against the pendulum decreases the pendulum's energy, damping its motion.

In the same way, at particular times of the ENSO cycle (which would be during the development of El Niño conditions), gusts of westerly wind act to force the southern oscillation deeper into El Niño, causing the developing event to become more intense. However, once an El Niño event is over and conditions are returning to normal or heading towards La Niña (which, as was mentioned earlier does typically happen straight after an El Niño period), a westerly wind will act to damp the system, causing it to lose energy and so the following La Niña event (if the system has enough energy to get that far) is going to be of a lower intensity.

The analogy does help to explain why the 1997-98 El Niño event was so intense. These westerly winds, in all probability, do not last long enough on their own in order to drive one single oscillation to such a large intensity. The westerly winds usually come in relatively short bursts of varying intensity, length and timing. However, certain wind patterns that cause the system to resonate, can result in the amplification of the effective magnitude of the wind involved, giving the ENSO system a lot of energy, creating a very intense event. It has been said that ENSO is driven by a reinforcing feedback of conditions between the ocean and the atmosphere in the Pacific.

This pendulum analogy, while useful in discussing the dynamics and mechanism of ENSO which makes it impossible to predict accurately (just like the motion of the pendulum in the wind is impossible to predict accurately due to the inherent impossibility of predicting when such gusts will blow, and their strength) does have several flaws which must be considered.

The first flaw is the one-sided damping the pendulum must experience in order to accurately model ENSO. ENSO usually overshoots when recovering from El Niño to La Niña, but it very rarely goes directly from La Niña without a significant period (typically in the order of 1-2 years, but can be a few months) of neutral conditions in between. This flaw can easily be addressed by asserting that the normal wind experienced by the pendulum in the analogy is not still air, but a slight easterly breeze, subject to random easterly and westerly gusts induced by turbulence. This means "neutral" for the pendulum is in fact leaning slightly to the west, instead of being at rest at the equilibrium point as would be the case for a pendulum in still air. This is analogous of the fact that under normal conditions, the air in the Pacific is not still, but rather blowing in an easterly direction. This wind of course, is the Trade Winds that were mentioned earlier. This normal slight easterly wind in the pendulum analogy also acts to slow down motion to the east while it prevents the motion losing energy sufficiently to allow the overshoot when going towards La Niña conditions, providing the required one-sided damping. This normal slight easterly wind also adds to the model the fact that when the pendulum is in a neutral position, a sufficiently short and/or weak westerly burst which does not give the pendulum much energy will not result in El Niño, the easterly wind is restored in time to return the pendulum back to its neutral position before it travels too far to the east. Likewise, in ENSO, after a small westerly burst, the trade winds prevent the water which is released to the east from going too far, and the system recovers before an El Niño event can occur.

The second flaw is more fundamental. In ENSO, the "weight" is a fluid. It can vary in mass quite easily, just by varying the amount of surface water that is allowed to move to the eastern and western sides of the Pacific. However, in the pendulum analogy, the weight is solid and of constant mass. This means that ENSO has an extra mode to its oscillation than the pendulum does - a pendulum is limited to one mode of oscillation - swinging in an arc. However

ENSO can oscillate by moving a large body of water from side to side (this is most reminiscent to the pendulum's motion), or it can release small amounts of fluid in response to turbulent gusts of wind, changing the mass of the fluid at the east or the west of the Pacific (something a simple, or even a physical pendulum cannot readily do), or it could even have multiple large bodies of water of similar size and therefore mass, travelling across the Pacific at the same time. The pendulum can only be an analogue to the centre of mass of the water in the Pacific, which when the motion of water as a whole is approximated, is not likely to be as simple as a simple pendulum. Maybe a pendulum with more modes of oscillation, such as a swinging swing (an analogy Peter Lynch considered in his paper regarding Rossby triads [9]), which has a radial component to the oscillation as well as the tangential component, or a double pendulum, which has a second pendulum hanging off the weight of the first pendulum, could more accurately model ENSO. Researchers should definitely investigate such models further.

There are several other factors the pendulum model fails to account for. The Pacific Ocean is not of constant depth, or even of a depth profile that can readily be modelled by a simple function. There are land masses that the water must negotiate a path around as it migrates from one side of the Pacific to the other. As the water travels in the form of waves initiated by the wind, this typically results in diffraction, which brings about some out-of-plane (meridonal) motion, so to account for this fact, if the pendulum in the model is to be more than a simple approximation, it needs to have some small obstacles in its path that are going to deflected slightly out of the plane, but this out of plane deflection is going to have to be extremely small, as landmasses are typically much smaller than the width of the Pacific, and therefore the arc of the pendulum. These obstacles can be safely neglected for most approximation purposes.

But this only accounts for the land masses that breach the surface of the

ocean. There are other land masses that affect the motion of the water. It will typically travel in the form of gravity waves, and for gravity waves the speed is dependent on the depth of the water - deeper water yields faster waves. The seabed is not a smooth item - it has some large ridges and crevasses in places. It is impossible to know its exact profile without measuring it, possibly by sonar, or a similar method. Even once these measurements are done, it's not obvious exactly how the variability of the sea bed corresponds to the pendulum analogue. But it has to have some effect - varying the speed of the waves is going to change the time at which the water reaches the edge of the Pacific, which is going to affect the iming of ENSO events. And the whole purpose of the exercise is to offer a relatively simple model of ENSO that still provides an accurate analogue of the system, in order to draw some inferences about its predictability.

Chapter 7

Summary

We have reviewed the equations of the atmosphere from a fluid dynamical context. We obtained equations of state for both dry air and wet air. The heat capacity of the air has been discussed and the requirements for stability in the atmosphere have been analysed in the cases of both a saturated atmosphere and an unsaturated atmosphere.

Several quantities that describe the degree of rotation in the fluid, namely the circulation and the vorticity, have been studied, as well as the enstrophy, a quantity that can be obtained by integrating the square of the vorticity over volume.

We reviewed that the coriolis force, which has the effect of causing large bodies of fluid (i.e. bodies of fluid that are large in comparison to the Rossby Radius of Deformation) to rotate relative to the earth's surface, depends on the coriolis parameter. The coriolis parameter varies with latitude in a manner that over, a very small range of latitudes, can be thought of as a constant. This is the f-plane approximation. For slightly larger ranges of latitude, a more appropriate approximation is the beta-plane approximation, where the coriolis parameter varies with latitude in a linear manner.

Rossby waves in the atmosphere, a form of slow moving wave with a large wavelength and therefore a large period, were studied. The dispersion relation of these waves in the case of a barotropic atmosphere, were obtained. This allowed us to find an expression for the phase speed and the group speeds of Rossby waves, which we did in both the meridonal direction and the zonal direction. We analysed a model by Peter Lynch [9] which compared a resonant Rossby wave triad to a swinging spring and found the two systems to be very different physically, but both systems obey the same governing equations. This inspired a simulation where we found that found that resonant Rossby triads are unstable, by way of adding different amplitudes of noise to a resonant Rossby triad and finding that larger quantities of noise result in an earlier arrival at instability.

Then we studied a different kind of Planetary wave, a Kelvin wave. We found there are two media in which Kelvin waves exist - the ocean and the atmosphere. We also saw that the equator acts as a waveguide for Kelvin waves and there are both surface and internal Kelvin waves.We found the equation of oceanic equatorial Kelvin waves, and found the form of atmospheric Kelvin waves, which depends on the height in an unspecified manner.

We studied the El Niño Southern Oscillation, including a discussion of the mechanism which leads to El Niño and La Niña, which influence the weather in the eastern and western sides of the Pacific Ocean. We discovered why it is impossible to accurately predict the ENSO cycle and compared the ENSO cycle to a pendulum swinging in a breeze.

References

[1] Ahrens, C. Donald, *Meteorology Today: An Introduction to Weather, Climate and the Environment (8th Edition)*, Thomson Brooks/Cole (2007), p. 327

[2] Australian Bureau of Meteorology, `http://www.bom.gov.au/climate/current/soihtm1.shtml`, Accessed 22 March 2011.

[3] Gill, Adrian, *Atmosphere-Ocean Dynamics*, Academic Press, USA (1982)

[4] Federov, A. V. et al, *How Predictable is El Niño?*, American Meteorological Society, July 2003

[5] Graebel, W. P., *Advanced Fluid Mechanics*, Academic Press, USA (2007)

[6] Holten, James and Lindzen, Richard, *A Note on "Kelvin" Waves in the Atmosphere*, Monthly Weather Review, June 1968

[7] Lindzen, Richard, *Planetary Waves on Beta Planes*, Monthly Weather Review, July 1967

[8] Lorenz, Edward, *Does the Flap of a Butterfly's Wings in Brazil Set Off a Tornado in Texas*, Conference, American Assosciation for the Advancement of Science, 1972

[9] Lynch, Peter, *Resonant Rossby Waves and the Swinging Spring*, Bulletin American Meteorological Society, November 2001

[10] Pedlosky, Joseph, *Geophysical Fluid Dynamics*, Springer Press, 1987

[11] Rossby, Carl-Gustaf, *Relation Between Variations in the Intensity of the Zonal Circulation of the Atmosphere and the Displacements of the Semi-Permanent Centres of Action*, Journal of Marine Research, 1939

[12] Roux, Filippus S., *Fluid dynamical enstrophy and the number of optical vortices in a paraxial beam*, Science Direct, 2006

[13] Sakagami, Taichiro, *El Niño*, video series, Nicholas School of the Environment, Duke University (2009)

[14] Thomson, William, *On Gravitational Oscillations of Rotating Water*, Proceedings of the Royal Society of Edinburgh, 1879

[15] Vallis, Geoffrey K., *Atmospheric and Oceanic Fluid Dynamics*, Supplementary Material for Second Edition, 2012 `www.princeton.edu/~gkv/aofd/aofdeqoce.pdf`, Accessed 16 February 2012

[16] World Meteorological Organisation, *The 1997-98 El Niño Event in Brief*, `www.wmo.net/pages/prog/wcp/wcdmp/relatedpubs/pdf/El_Nino_in_Brief.pdf`